NASA Technical Memorandum 86450

Theoretical and Experimental Flow Fields for a Supersonic Cruise Fighter Forebody

Steven F. Yaros

NOVEMBER 1985

NASA Technical Memorandum 86450

Theoretical and Experimental Flow Fields for a Supersonic Cruise Fighter Forebody

Steven F. Yaros
Langley Research Center
Hampton, Virginia

National Aeronautics
and Space Administration

**Scientific and Technical
Information Branch**

1985

INTRODUCTION

The study of airframe and engine-inlet integration has recently become even more important in the light of current supersonic cruise fighter ("supercruiser") aircraft design. These configurations are characterized by fuselages and canopies with distinctly nonaxisymmetric cross-sectional geometries and thin, low-aspect-ratio, highly tapered swept wings. Such aircraft configurations may also include, in more complicated cases, forward-mounted canards, leading-edge extensions, fins, and stores hung in a multitude of combinations. Such configurations present many problems in the world of airframe/inlet design (refs. 1 to 4), particularly the accurate prediction of the flow field about the aircraft forebody.

Since propulsion models are generally complex and very expensive, most design teams do not conduct propulsion testing until the external lines of a configuration are fairly well established. Thus it is necessary to develop accurate computational methods that can be used to assess inlet flow-field effects before aircraft configurations are fully defined. The purpose of this paper is to investigate the capability of three inviscid methods to predict the flow about a supercruiser configuration at several transonic Mach numbers and several angles of attack.

The speed range from Mach 0.6 to Mach 1.2 and angles of attack from 0° to 10° were of interest because of the wind-tunnel data, and of prime importance was the realistic modeling of the aircraft geometry. The ease of use of the computer programs that implemented each method and their economy of operation were also considered.

Predictions of aircraft forebody flows are valuable not only to the designer but also to the wind-tunnel test engineer (ref. 5). The results are presented in a form particularly useful to both, namely, flow-field contours of local angle of attack, local angle of sideslip, and local Mach number at a hypothetical inlet entrance plane. Similar results have been presented in reference 6 for more standard fighter configurations. This report is a continuation of that effort for a more sophisticated aircraft configuration. In addition, the predictions and data herein include a more extensive flow-field area than was defined in reference 6.

SYMBOLS

M	Mach number
u,v,w	total velocities corresponding to x-, y-, and z-directions
x,y,z	Cartesian coordinates in aircraft axial, transverse, and normal directions
α	angle of attack, $\tan^{-1}(w/u)$
β	angle of sideslip, $\tan^{-1}(v/u)$

Subscripts:

l	local conditions
∞	free-stream conditions

NUMERICAL PREDICTION METHODS

Because of the differences in the simplified equations of motion for supersonic and transonic flows, almost all the numerical methods investigated were specifically for one speed regime or the other. During the course of this study, certain criteria were used to assess the applicability of each of the computer programs. Solution accuracy, integrity of the geometric model, operational ease, and running expense were the most important criteria. In the final analysis, for supersonic speeds, a three-dimensional Euler equation "marching" code, STEIN, was chosen over other codes (refs. 7 and 8).

A similar situation developed in the search for a transonic code. Ultimately, a small-disturbance code, WIBCO (wing-body code), was chosen over a full-potential code, FLO-30, which is a member of a family of FLO codes (refs. 9 to 12) that are capable of solutions for fuselages of only moderate complexity, particularly if the wing is of low aspect ratio. Since many of the fighter cross sections varied considerably from an axisymmetric shape, it was decided that WIBCO, having a more flexible geometry package, would be the better choice, in spite of the small-disturbance approximations applied in the calculations.

One other factor weighed heavily in the choice of the STEIN code and WIBCO: the similarity of the aircraft model geometry input. Both codes have slightly different versions of the QUICK-geometry methodology developed by Vachris and Yager (ref. 13). In this method, the aircraft cross sections are described at appropriate fuselage stations by specifying the control points and the types of curves to be used to connect the points. After the details of each cross-sectional geometric model are specified, the longitudinal aircraft body lines are described in a manner similar to the cross sections, piece by piece, with analytic functions. This task is made easier through the use of interactive design codes (refs. 14 and 15). The result is an analytic body model that allows a quick calculation of surface points and slopes over the entire length of the body.

The STEIN code is fully described in references 16 and 17. Although the version of STEIN used was the latest, as presented in reference 18, and had been used to predict many of the flows in reference 6, the basic nature of the code was incompatible with the flight conditions of the wind-tunnel tests. Because of the model geometry and relatively low Mach numbers tested, large regions of subsonic flow were almost always present, particularly near the canopy-fuselage and wing-fuselage junctures. This situation made it impossible for the STEIN code to march through these areas, particularly for free-stream Mach numbers below 1.6. Thus, no STEIN prediction compatible with the data can be presented herein.

The WIBCO transonic code was developed by Boppe (ref. 19) primarily to apply the solution of the small-disturbance potential equation to arbitrary wing and body geometries. Recognizing the increasing complexity of traditional grid transformations as configurations become more three-dimensional, Boppe avoids these problems by imbedding fine Cartesian grids into an overall coarse grid in regions where

more flow detail is required. The crude grid in the physical space is stretched in all directions to infinity (except at the plane of symmetry) according to the method of reference 20. Stretching in the z-direction is also proportional to the tangent function, whereas in the y-direction, the stretching function is the hyperbolic tangent.

The wing and body fine-grid systems are constructed to totally encapsulate their portions of the geometry and to provide computations over a much smaller area of the flow. These two fine-grid systems overlap and transfer information to each other, as well as to the crude-grid system, during the course of the iterations. It should be noted that although the body fine-grid system is a regular Cartesian grid, the wing fine-grid system is swept and tapered according to the planform shape.

The finite-difference approximations are straightforward. Central differencing is used throughout except in areas of local supersonic flow, in which upwind differencing is used for most of the second-derivative terms. In keeping with the near-isentropic nature of the flow, nonconservative difference operators are used, although it is acknowledged that results will become less accurate with increasing shock strength. For a wing-body configuration, the solution begins with an arbitrary number (typically 100) of successive line-overrelaxation sweeps of the crude grid to provide a starting solution for the fine-grid systems. The second phase of the solution involves a sweep of the wing fine-grid system, the body fine-grid system, and the crude-grid system, with appropriate updating of overlapping areas. Approximately 80 second-phase iterations are usually required. Since none of the grid systems are body or wing fitted, boundary conditions are applied at mesh points nearest the actual surfaces. Corrections are applied at these points for wing-surface slope and body displacement as well as for local flow inclination. Rate of convergence is measured by the decrease in changes in the potential function.

The version of WIBCO used herein is the basic wing-body code. Further capabilities have been added (ref. 21), including the fine-grid system applied to pylons, nacelles, and winglets, as well as a scheme for modeling inlet spillage and exhaust interference effects. In addition to the individual references for the two methods (refs. 16 to 21), a more detailed explanation of the methods and how they are used is presented in references 6 and 22.

A comparison run using a third computer code from Shankar and Szema was made. The code, described in reference 23, is a recently developed numerical method based on the conservation form of the full-potential equation. It is limited to three-dimensional supersonic flows, although the marching technique normally used is switched to a relaxation algorithm in areas of localized subsonic flow. Because of this limitation, this method was used only for the highest Mach number, 1.2, at the highest angle of attack tested, 7.5°.

EXPERIMENTAL DATA

Wind-tunnel tests were performed in the Langley 16-Foot Transonic Tunnel to provide a data base for comparison with the results of the computer code used in this study. The aircraft model, built by the Boeing Military Airplane Company, was designed to be representative of a typical supersonic tactical aircraft configuration. The model itself had been tested previously for various purposes (refs. 24 and 25), primarily nacelle/nozzle integration studies. The aircraft

configuration consists of a fighter-type fuselage with a low-aspect-ratio, highly swept, tapered wing, which is evident from a photograph of its installation in the wind tunnel (fig. 1). Three types of data were taken during the wind-tunnel tests (ref. 26):

Flow-field (cone probe) data at three representative inlet locations

Wing and fuselage boundary layer data

Wing static pressures

For purposes of code comparison, the flow-field data, which include local angle of attack, local angle of sideslip, and local Mach number, were used, as they were with Tailor-Mate data in the theory assessment in references 6 and 22. Results are presented for the upper and lower aft data positions, which are at the same fuselage station above and below the wing, since most of the flow-field data were taken in these areas. The location of the aft measurement area is indicated in figure 2, which is a representation of the body and wing geometry generated in WIBCO. Data were taken in a matrix of three Mach numbers and three angles of attack: $\alpha = 0^{\circ}$, 5°, and 10° for $M_{\infty} = 0.6$ and 0.9 and $\alpha = 0^{\circ}$, 5°, and 7.5° for $M_{\infty} = 1.2$.

These wind-tunnel data have also been presented in references 27 and 28. An abbreviated summary of the flow predictions herein is available in reference 27.

RESULTS AND DISCUSSION

WIBCO, based on the geometric model shown in figure 2, was capable of generating solutions for all nine points in the Mach number/angle-of-attack test matrix. The results of the solutions are shown in figures 3 to 11. Results are judged according to both the qualitative and quantitative agreement of the predicted contour lines with the wind-tunnel data. Examination of the $\alpha = 0^{\circ}$ data shows good agreement in local angles of attack and sideslip at all three Mach numbers. As in the theory assessment of references 6 and 22 using the Tailor-Mate data, agreement is only fair in the Mach number contours, but at this angle of attack, the Mach number change is so low that comparison of contours may be misleading. Angular predictions generally agree with experimental values withn 1°, a figure that indicates a lack of any strong viscous effects at this angle of attack.

In figures 6 to 8, all at $\alpha = 5^{\circ}$, the experimental local angles of attack and sideslip both exhibit more variation than the predicted values. This effect increases strongly with increasing Mach number and is especially noticeable in the greatly increased inflow over the wing. Experimental data and predicted values agree within 2° in general, except at a Mach number of 1.2 (fig. 8), where the formation of an upper surface vortex is indicated. Local experimental Mach number distributions become more varied as the free-stream Mach number is increased, a result of wing leading-edge vortex formation and a possible upstream shock wave at the highest Mach number.

The pattern of the flow becomes apparent in the last series of data, figures 9 to 11, where the free-stream angles of attack were $\alpha = 10^{\circ}$ for $M_{\infty} = 0.6$ and 0.9 and $\alpha = 7.5^{\circ}$ for $M_{\infty} = 1.2$. Examination of the local sideslip

angles indicates extremely strong inflow angles in the data close to the wing, a condition which may indicate a well-developed leading-edge vortex traversing the flow-field area. Above the wing, angle-of-attack contours are much more dense than WIBCO predicts, and as free-stream Mach number increases, the Mach contours again vary substantially, most likely as a result of vortex and/or upstream shock wave formation (ref. 26). Local flow angles predicted are, in fact, so different from the experimental data as to indicate an entirely different flow pattern above the wing.

It is not surprising that a wing this highly swept would develop a leading-edge vortex at such moderate angles of attack. Nor is it surprising that WIBCO would not predict such a vortical development, for codes capable of doing such include, in some manner, viscous effects. Although WIBCO is partially unsuccessful in these cases, the predictions below the wing where the flow is much better behaved are reasonable in most cases.

The results of the full-potential code of Shankar and Szema are shown in figures 12(a) to 12(c) in comparison with the WIBCO results. Good agreement, within 1°, in local angle of attack is apparent, with fair agreement, within 2°, in the local angle of sideslip. The Shankar code shows a more pronounced outflow pattern below the wing and a more pronounced inflow pattern above the wing in comparison with WIBCO. The Mach number patterns seem to be qualitatively similar, but numerical agreement is questionable. The two prediction methods agree more closely with each other than they do with the wind-tunnel data, as is apparent by comparing figure 12(c) with figure 11(c). This particular flight condition, Mach 1.2 and an angle of attack of 7.5°, was deemed to be at the limit of the capability of the Shankar and Szema code. Any decrease in Mach number or increase in angle of attack would produce such massive subsonic regions, as well as areas of detached shock waves, that the basic marching nature of the code would be impossible to carry out.

CONCLUDING REMARKS

Of the three codes that were examined for their capability of predicting forebody flows about a complex supersonic cruise fighter configuration, only two were successful. The supersonic Euler equation code STEIN failed to march past the leading edge of the wing below a Mach number of 1.6, which was greater than the Mach numbers for which wind-tunnel data were available. WIBCO, the small-disturbance transonic code, provided solutions at all the Mach numbers and at all the angles of attack tested in the tunnel: 0°, 5°, and 10° at Mach 0.6 and Mach 0.9 and 0°, 5°, and 7.5° at Mach 1.2. The criteria for comparison (contours of local angle of attack, local angle of sideslip, and local Mach number) showed that WIBCO was capable of predicting the flow angles at the lower angles of attack, but development of viscous effects reduced prediction accuracy at a high angle of attack. In general, flow angle prediction was more accurate qualitatively than Mach number prediction. The Shankar code ran successfully at Mach 1.2, although it was at the lower limit of its Mach number range. Results are comparable to the WIBCO predictions, particularly for local angle of attack.

For aircraft configurations that include canards, strakes, and more exotic fuselage geometry, the codes may not perform satisfactorily, particularly at high angles of attack or sideslip. Under such flight conditions, boundary layer buildup

cannot be neglected even when the flow remains attached. This situation suggests that the next step in the analysis of such configurations should include viscous effects.

In general, both WIBCO and the Shankar code may be considered useful for design applications, depending on the degree of accuracy required for the users' needs. However, as Mach number and/or angle of attack increases, both solutions become less accurate because of their lack of viscous effects and any mechanism to predict vortex development.

NASA Langley Research Center
Hampton, VA 23665-5225
July 29, 1985

REFERENCES

1. Surber, Lewis; Syberg, Jan; and Koncsek, Joseph: Performance of Highly Integrated Inlets for Supersonic Aircraft. Aerodynamics of Power Plant Installation, AGARD-CP-301, Sept. 1981, pp. 1-1 - 1-12.

2. Williams, T. L.; Hunt, B. L.; Smeltzer, D. B.; and Nelms, W. P.: Top-Mounted Inlet System Feasibility for Transonic-Supersonic Fighter Aircraft Applications. Aerodynamics of Power Plant Installation, AGARD-CP-301, Sept. 1981, pp. 2-1 - 2-17.

3. Surber, Lewis E.: Effect of Forebody Shape and Shielding Technique on 2-D Supersonic Inlet Performance. AIAA Paper No. 75-1183, Sept.-Oct. 1975.

4. Smeltzer, D. B.; Nelms, W. P.; and Williams, T. L.: Airframe Effects on a Top-Mounted Fighter Inlet System. AIAA J. Aircr., vol. 19, no. 12, Dec. 1982, pp. 1083-1087.

5. Surber, L. E.; and Stava, D. J.: Supersonic Inlet Performance and Distortion During Maneuvering Flight. Inlets and Nozzles for Aerospace Engines, AGARD-CP-91-71, Dec. 1971, pp. 25-1 - 25-18.

6. Yaros, Steven F.: Theoretical and Experimental Engine-Inlet Flow Fields for Fighter Forebodies. NASA TP-2270, 1984.

7. Ehlers, F. E.; Epton, M. A.; Johnson, F. T.; Magnus, A. E.; and Rubbert, P. E.: An Improved Higher Order Panel Method for Linearized Supersonic Flow. AIAA Paper 78-15, Jan. 1978.

8. Landrum, Emma Jean; and Miller, David S.: Assessment of Analytic Methods for the Prediction of Aerodynamic Characteristics of Arbitrary Bodies at Supersonic Speeds. AIAA-80-0071, Jan. 1980.

9. Caughey, D. A.; and Jameson, A.: Numerical Calculation of Transonic Potential Flow About Wing-Body Combinations. AIAA Paper No. 77-677, June 1977.

10. Caughey, David A.; Newman, Perry A.; and Jameson, Antony: Recent Experiences With Three-Dimensional Transonic Potential Flow Calculations. NASA TM-78733, 1978.

11. Caughey, D. A.; and Jameson, Antony: Recent Progress in Finite-Volume Calculations for Wing-Fuselage Combinations. AIAA Paper 79-1513, July 1979.

12. Verhoff, A.; and O'Neil, P. J.: Extension of FLO Codes to Transonic Flow Prediction for Fighter Configurations. Transonic Aerodynamics, David Nixon, ed., American Inst. Aeronaut. & Astronaut., Inc., c.1982, pp. 467-487.

13. Vachris, Alfred F., Jr.; and Yaeger, Larry S.: QUICK-GEOMETRY - A Rapid Response Method for Mathematically Modeling Configuration Geometry. Applications of Computer Graphics in Engineering, NASA SP-390, 1975, pp. 49-73.

14. Adams, Mary S.: Interactive Input for the QUICK Geometry System - User's Manual. NASA TM-81933, 1980.

15. Townsend, James C.: Use of Interactive Graphics To Analyze QUICK-Geometry. Supplement to NASA TM-83234, 1982.

16. Marconi, Frank; Salas, Manuel; and Yaeger, Larry: Development of a Computer Code for Calculating the Steady Super/Hypersonic Inviscid Flow Around Real Configurations. Volume I - Computational Technique. NASA CR-2675, 1976.

17. Marconi, Frank; and Yaeger, Larry: Development of a Computer Code for Calculating the Steady Super/Hypersonic Inviscid Flow Around Real Configurations Volume II - Code Description. NASA CR-2676, 1976.

18. Marconi, Frank; and Koch, Frank: An Improved Supersonic, Three-Dimensional, External, Inviscid Flow Field Code. NASA CR-3108, 1979.

19. Boppe, Charles W.: Transonic Flow Field Analysis for Wing-Fuselage Configurations. NASA CR-3243, 1980.

20. Boppe, C. W.: Calculation of Transonic Wing Flows by Grid Embedding. AIAA Paper No. 77-207, Jan. 1977.

21. Boppe, C. W.; and Stern, M. A.: Simulated Transonic Flows for Aircraft With Nacelles, Pylons, and Winglets. AIAA-80-130, Jan. 1980.

22. Yaros, Steven F.: Evaluation of Two Analytical Methods for the Prediction of Inlet Flow Fields in the Vicinity of Generalized Forebodies. AIAA-82-0959, June 1982.

23. Shankar, V.; and Szema, K. Y.: Nonlinear Potential Analysis Techniques for Supersonic Aerodynamic Design. NASA CR-172507, 1985.

24. Hutchinson, R. A.; Petit, J. E.; Capone, F. J.; and Whittaker, R. W.: Investigation of Advanced Thrust Vectoring Exhaust Systems for High Speed Propulsive Lift. AIAA-80-1159, June/July 1980.

25. Capone, Francis J.; and Reubush, David E.: Effects of Varying Podded Nacelle-Nozzle Installations on Transonic Aeropropulsive Characteristics of a Supersonic Fighter Aircraft. NASA TP-2120, 1983.

26. Yetter, J. A.; Salemann, V.; and Sussman, M. B.: Inlet Flow Field Investigation, Part I - Transonic Flow Field Survey. NASA CR-172239, 1984.

27. Reubush, David E.; Bare, E. Ann; Yaros, Steven F.; and Yetter, Jeffery A.: Flow-Field Investigation of a Supercruise Fighter Model. AIAA-84-1331, June 1984.

28. Reubush, David E.; and Bare, E. Ann: Investigation of a Supersonic Cruise Fighter Model Flow Field. NASA TM-86361, 1985.

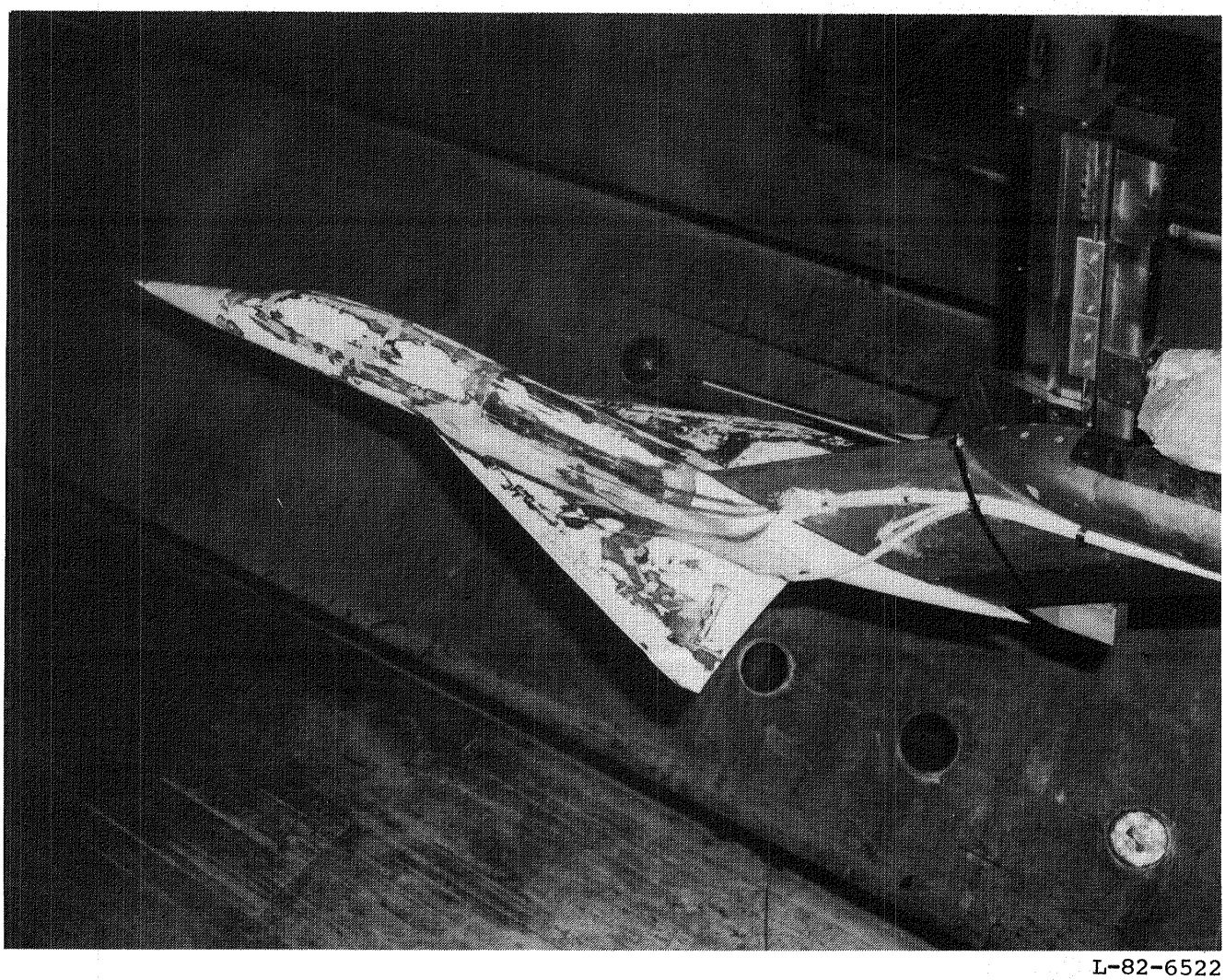

L-82-6522

Figure 1.- Supersonic cruise fighter model in the Langley 16-Foot Transonic Tunnel.

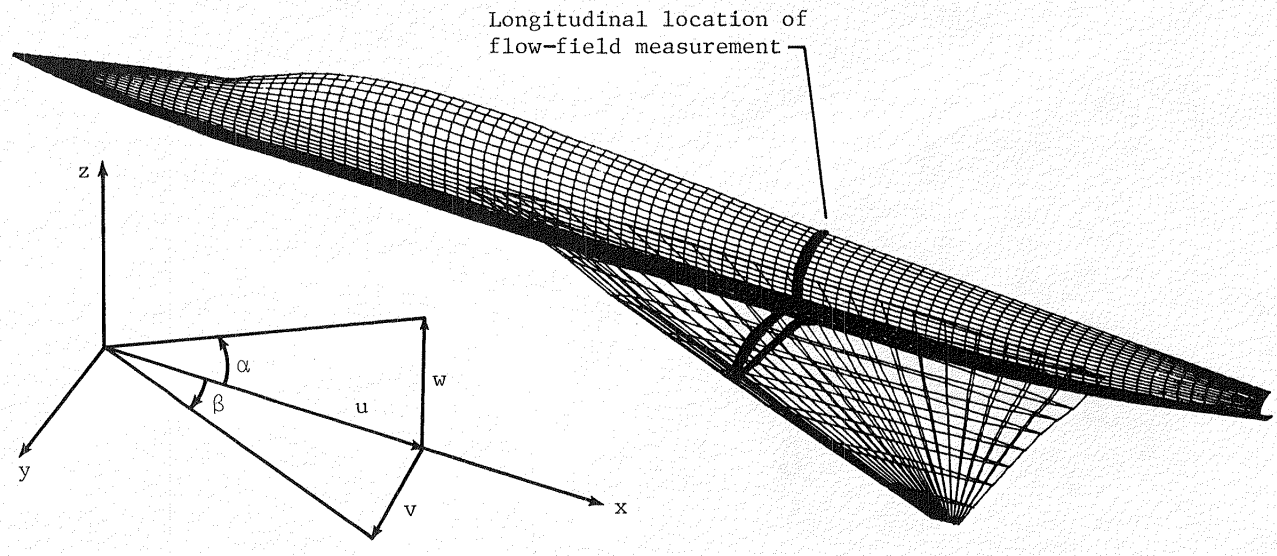

Figure 2.- Quick-geometry model of supersonic cruise fighter configuration for use with WIBCO.

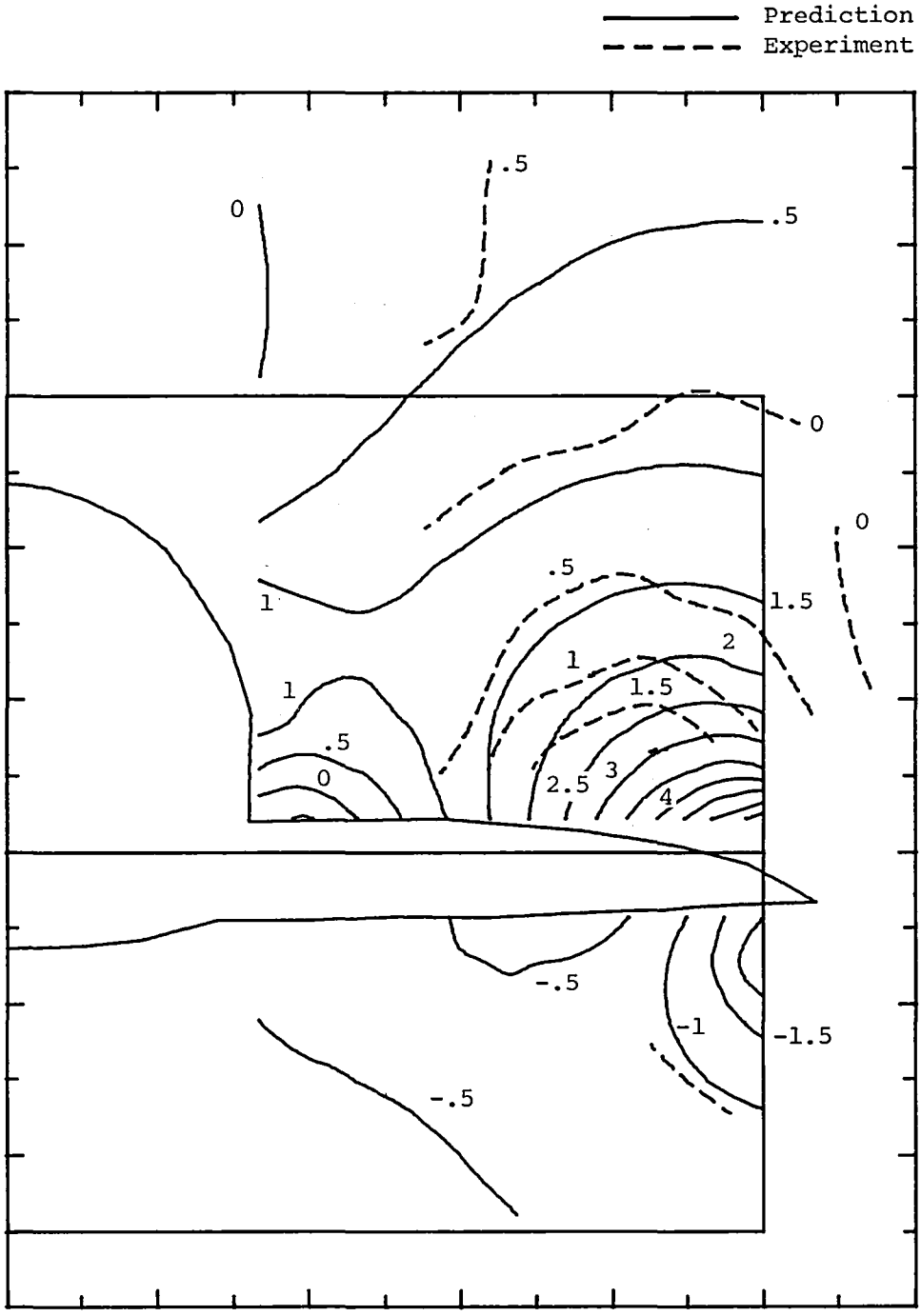

(a) α_l in degrees.

Figure 3.- Experimental contours and contours predicted by WIBCO at $M_\infty = 0.6$ and $\alpha = 0°$.

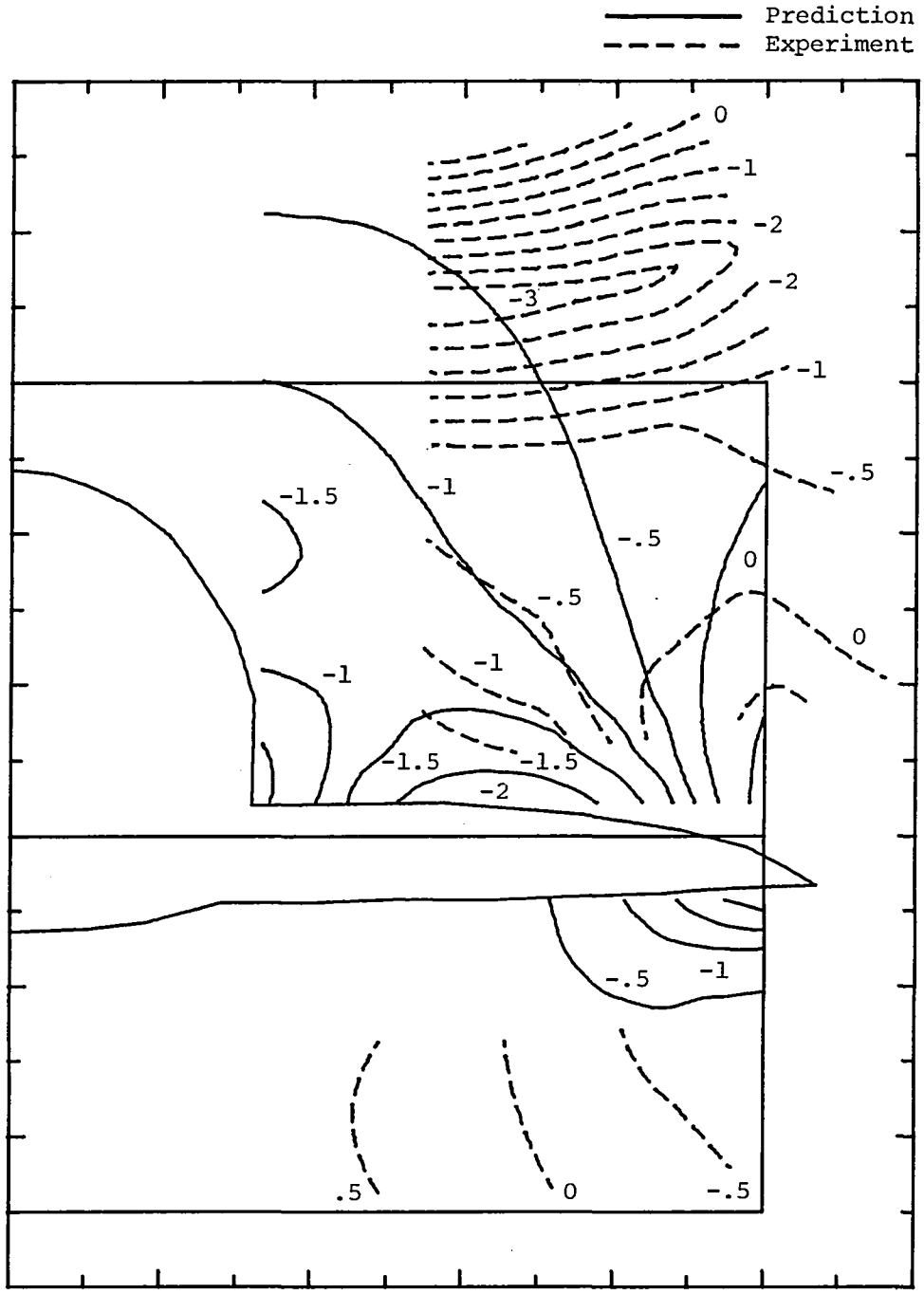

(b) β_1 in degrees.

Figure 3.- Continued.

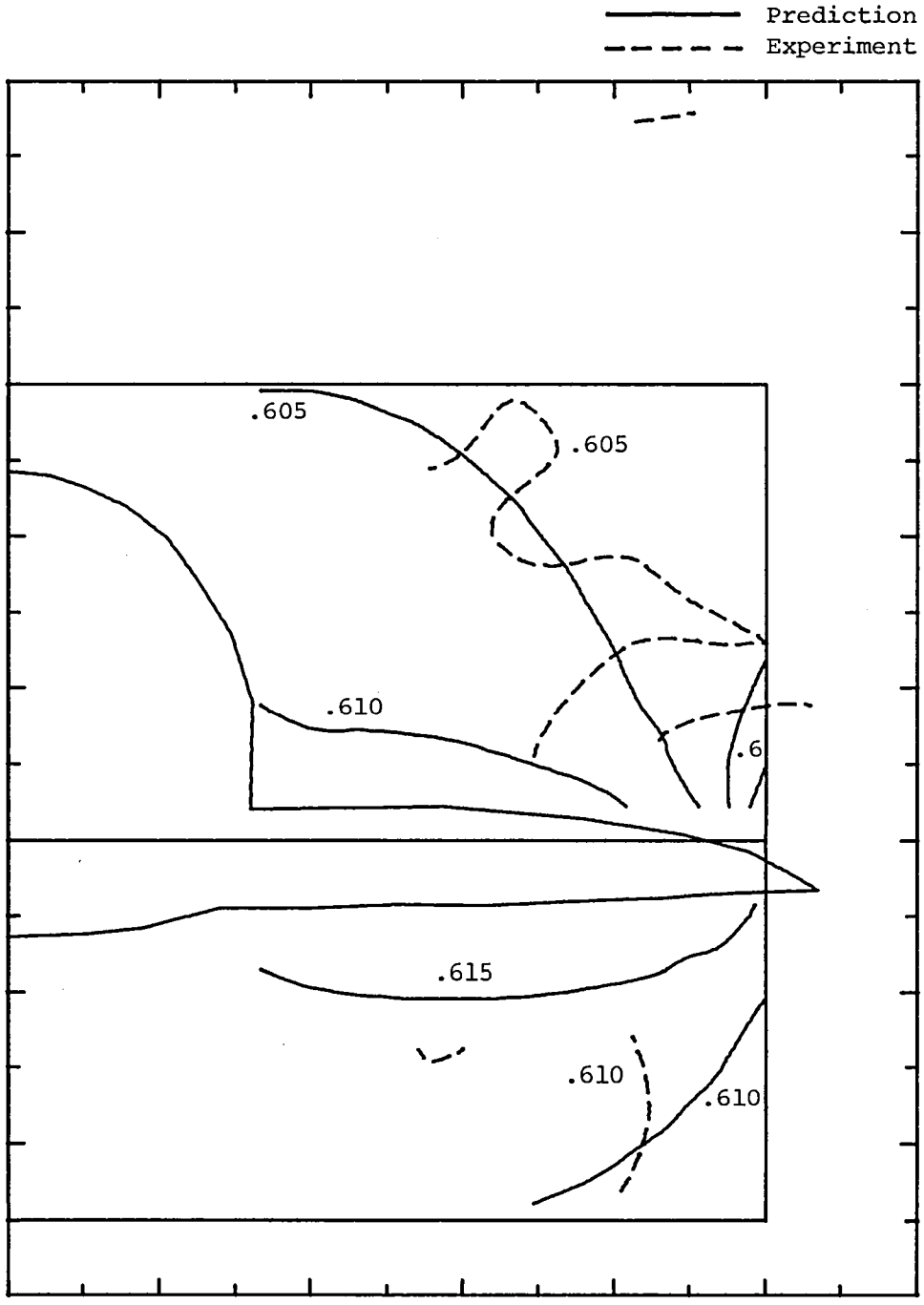

(c) M_1.

Figure 3.- Concluded.

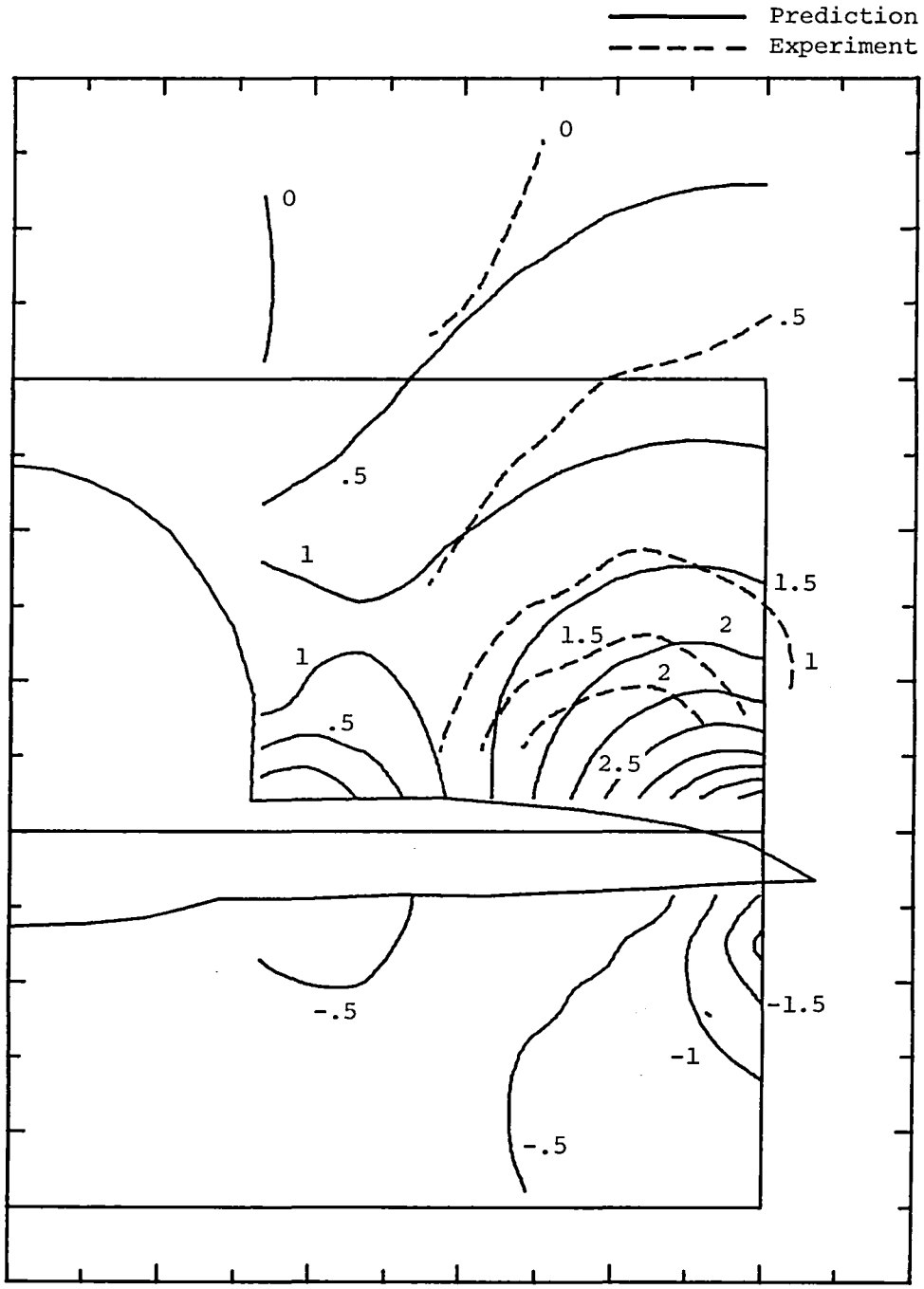

(a) α_l in degrees.

Figure 4.- Experimental contours and contours predicted by WIBCO at $M_\infty = 0.9$ and $\alpha = 0°$.

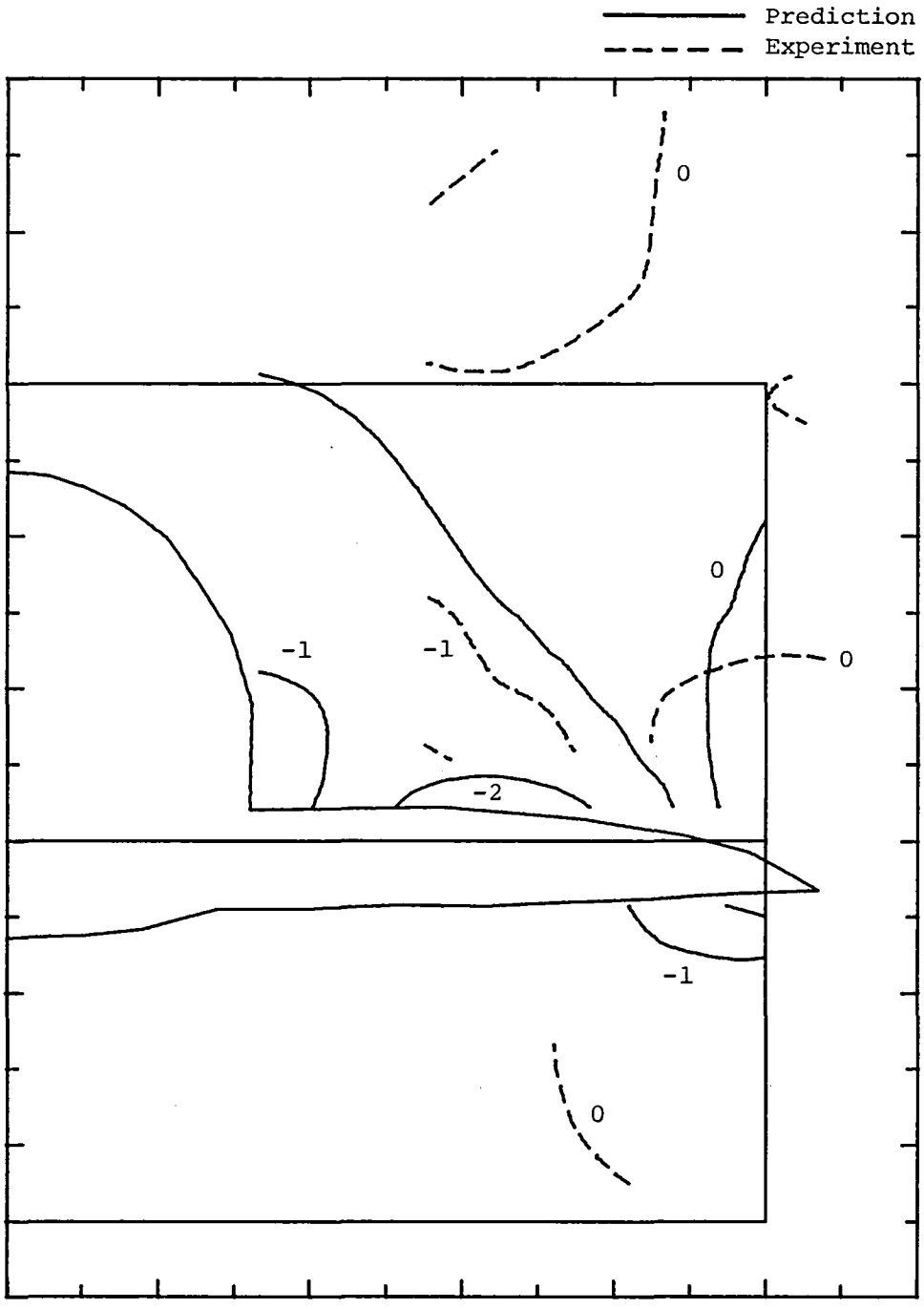

(b) β_1 in degrees.

Figure 4.- Continued.

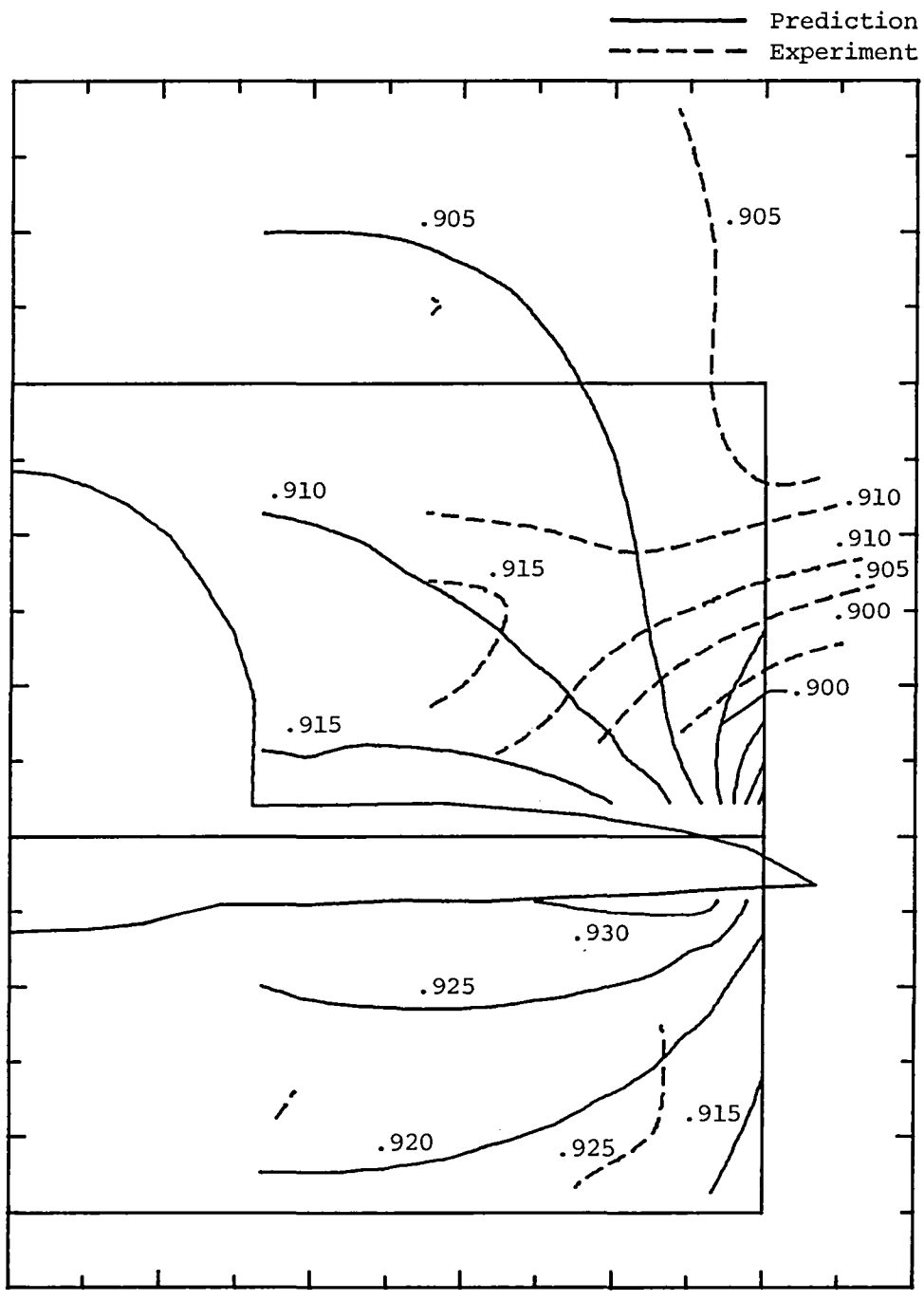

(c) M_1.

Figure 4.- Concluded.

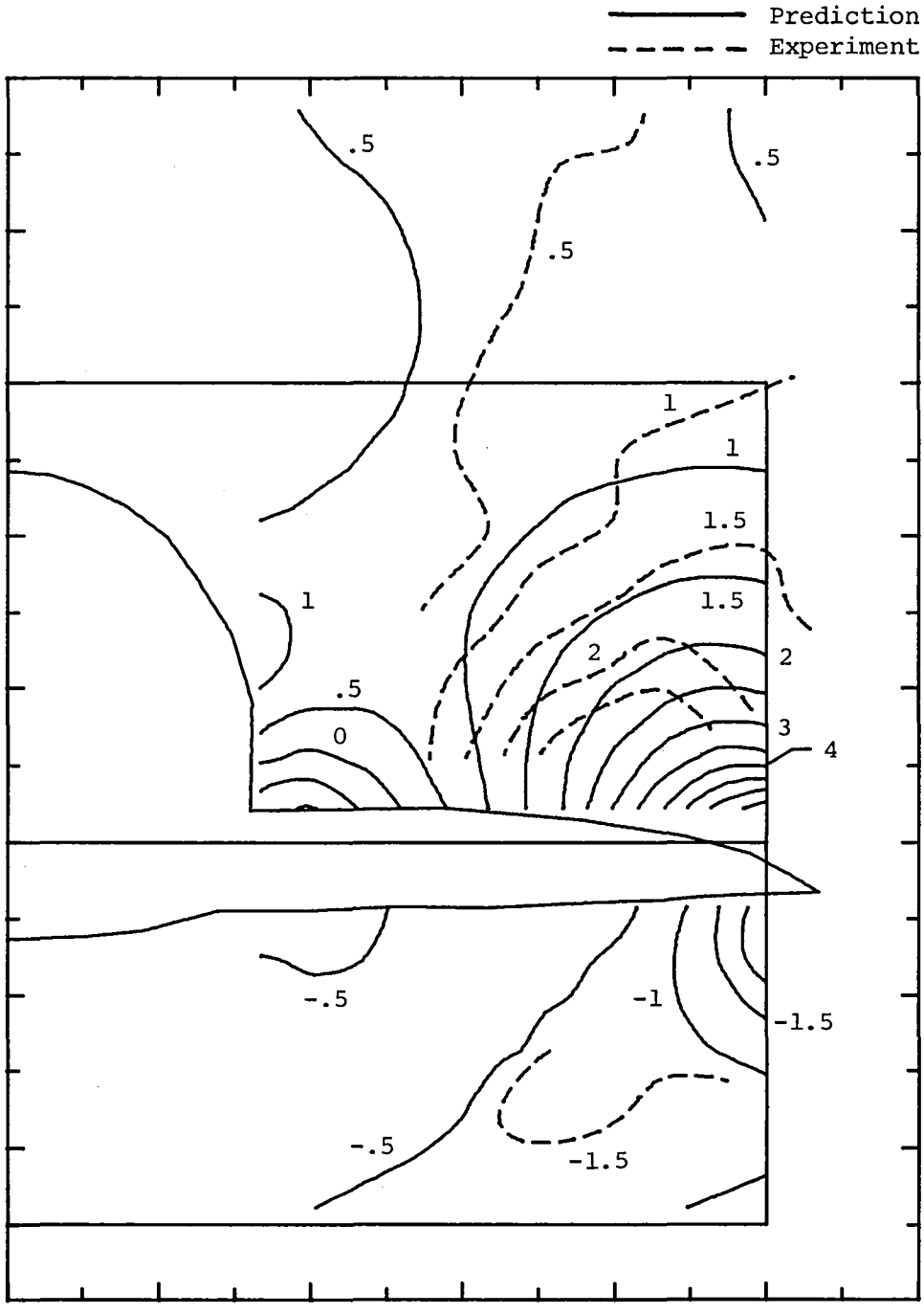

(a) α_l in degrees.

Figure 5.- Experimental contours and contours predicted by WIBCO at $M_\infty = 1.2$ and $\alpha = 0°$.

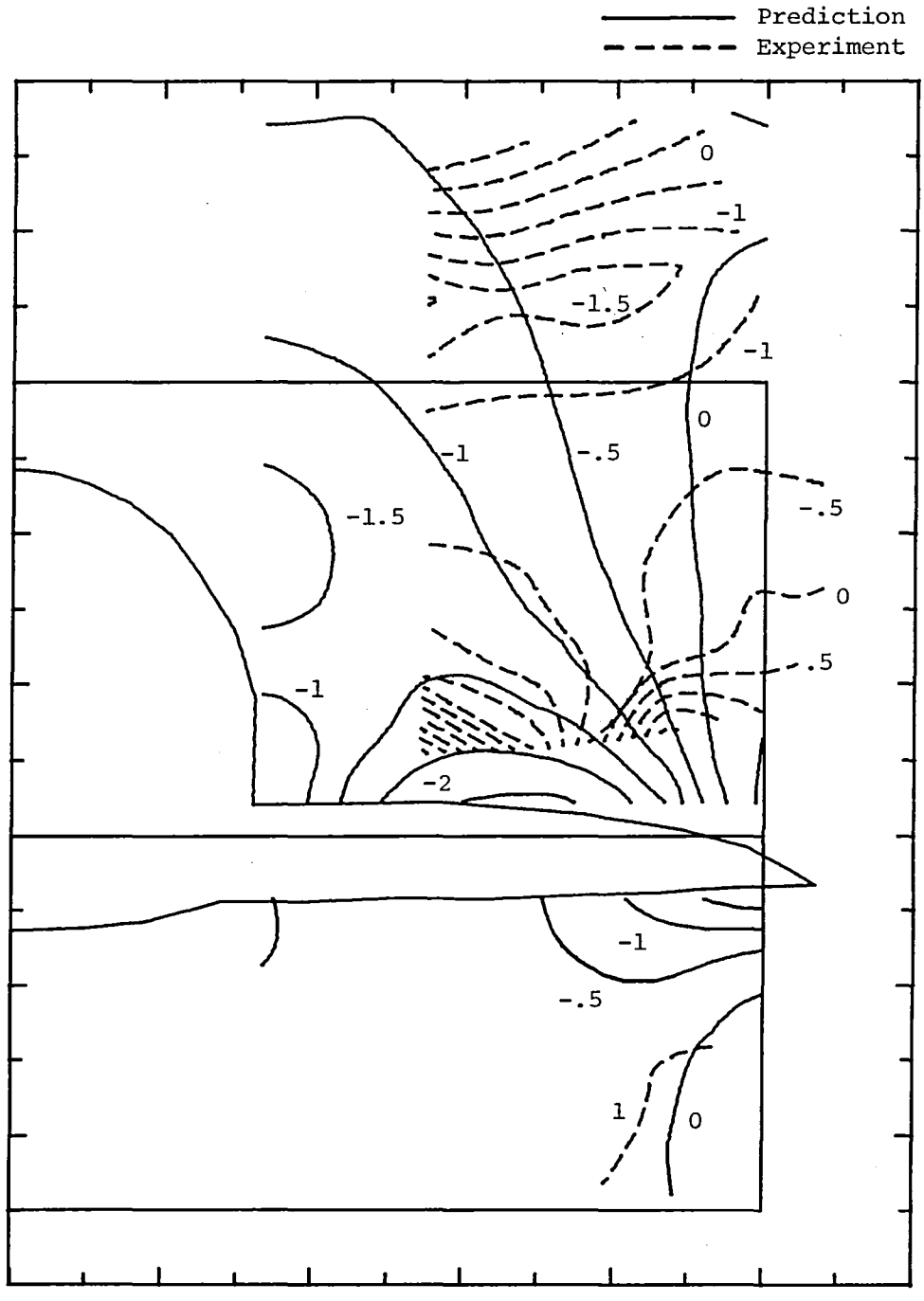

(b) β_1 in degrees.

Figure 5.- Continued.

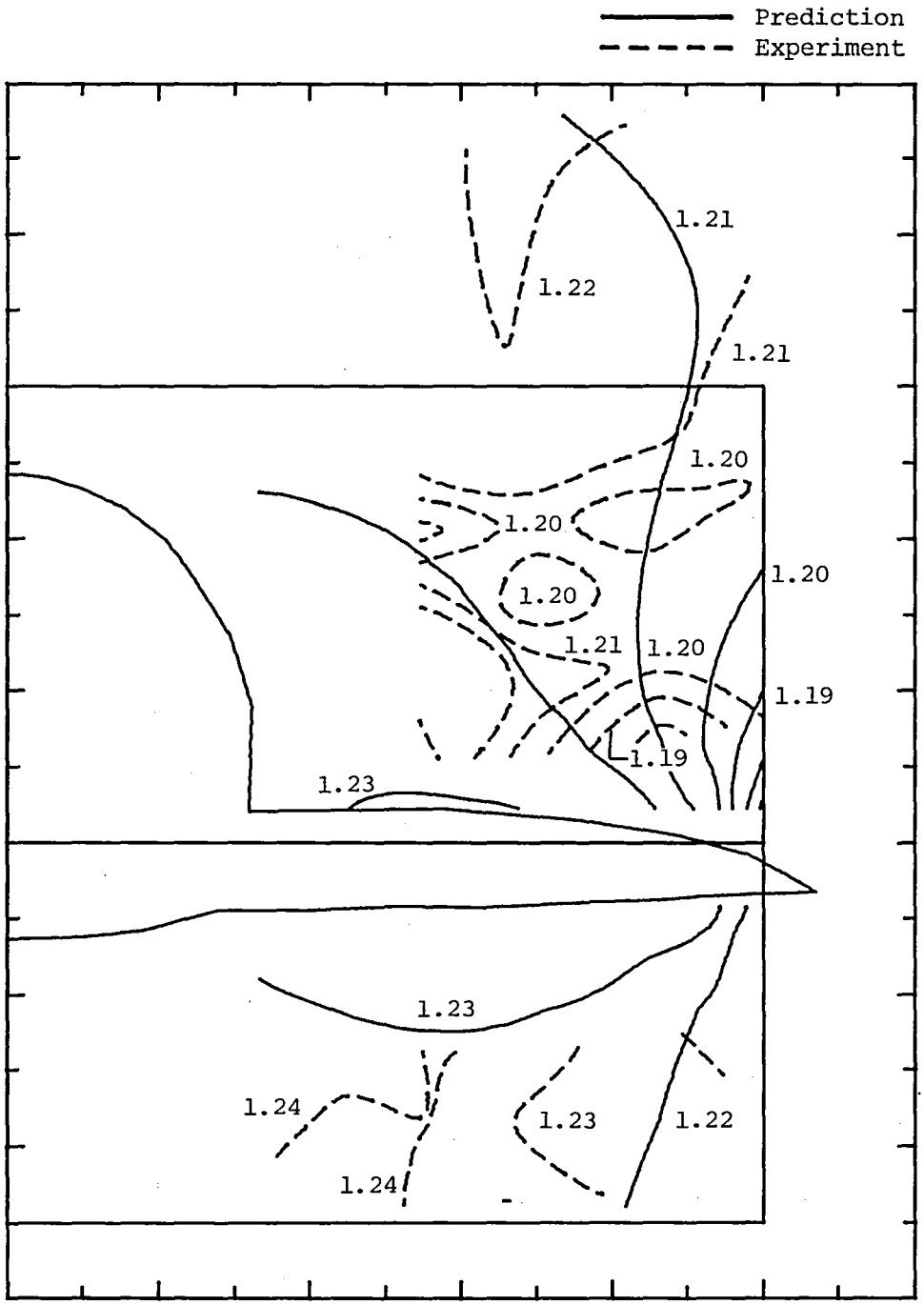

(c) M_1.

Figure 5.- Concluded.

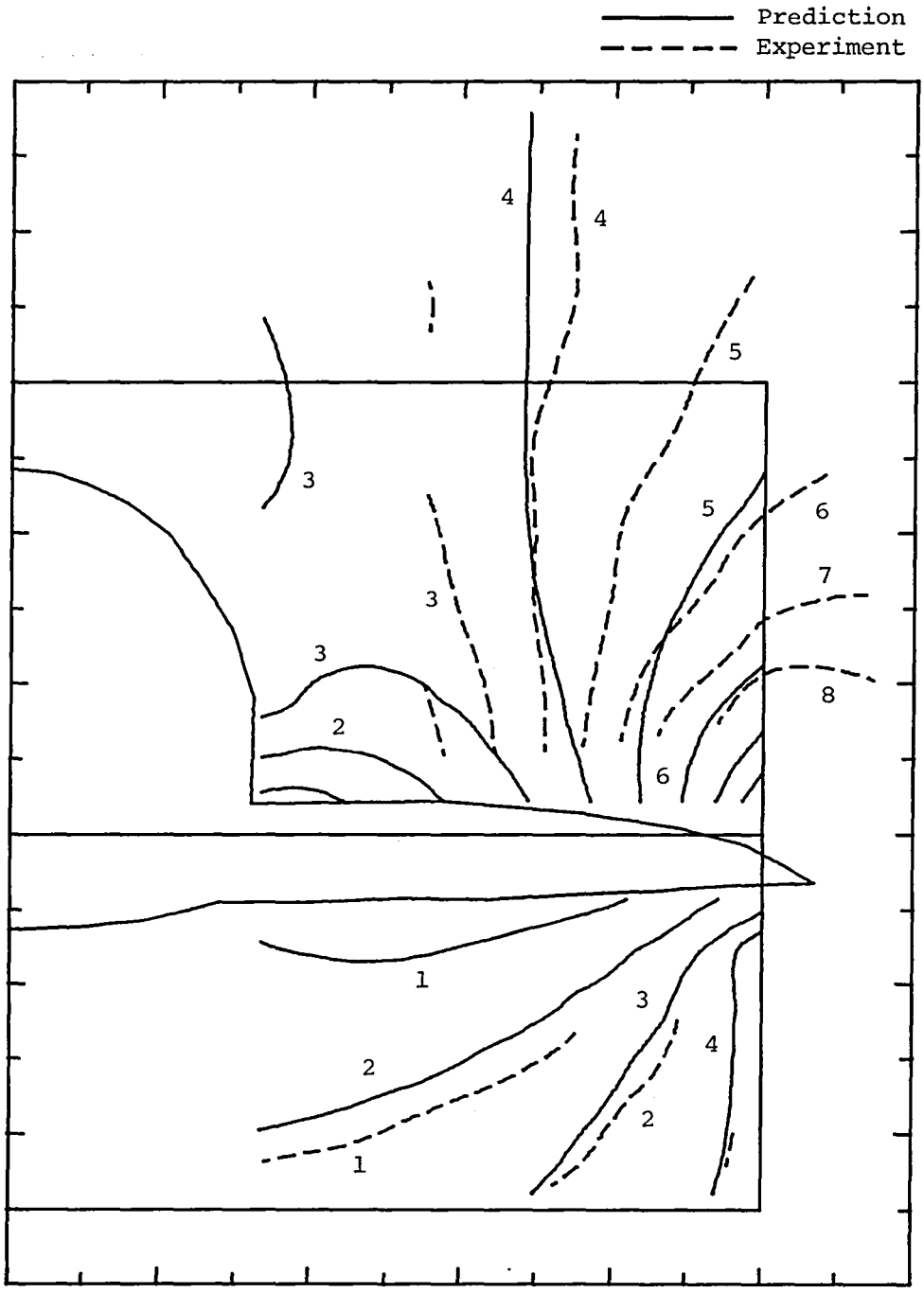

(a) α_i in degrees.

Figure 6.- Experimental contours and contours predicted by WIBCO at $M_\infty = 0.6$ and $\alpha = 5°$.

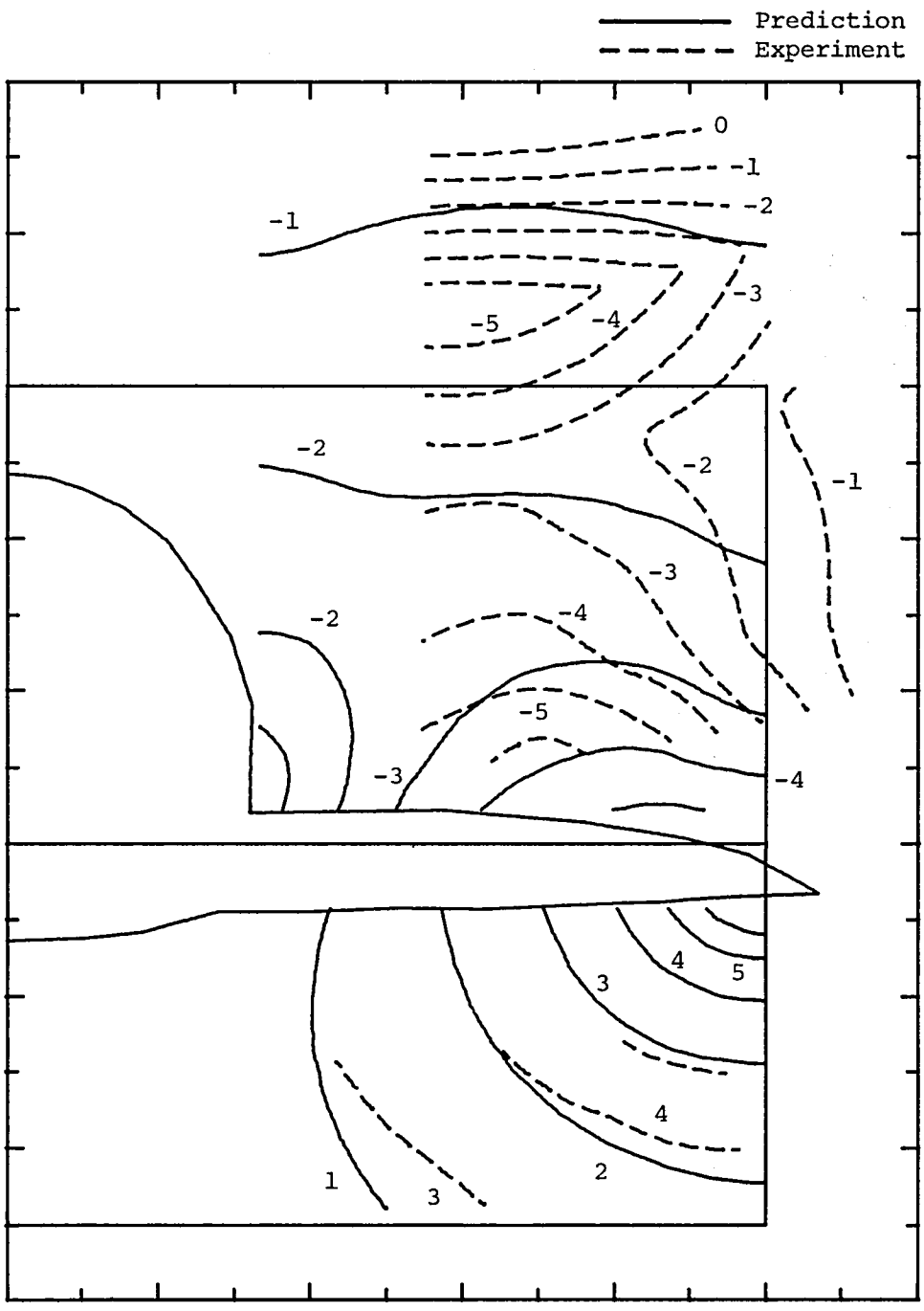

(b) β_i in degrees.

Figure 6.- Continued.

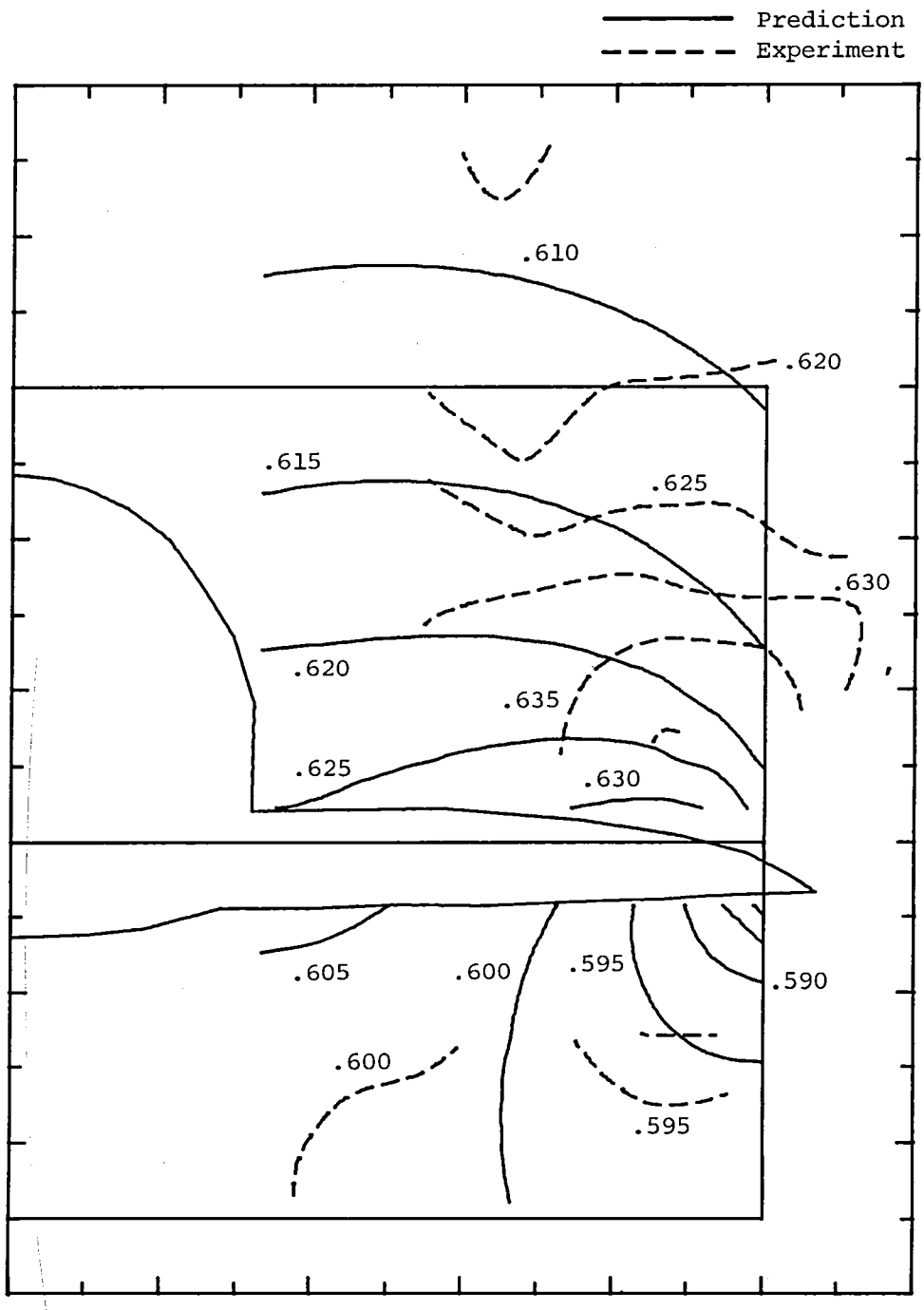

(c) M_1.

Figure 6.- Concluded.

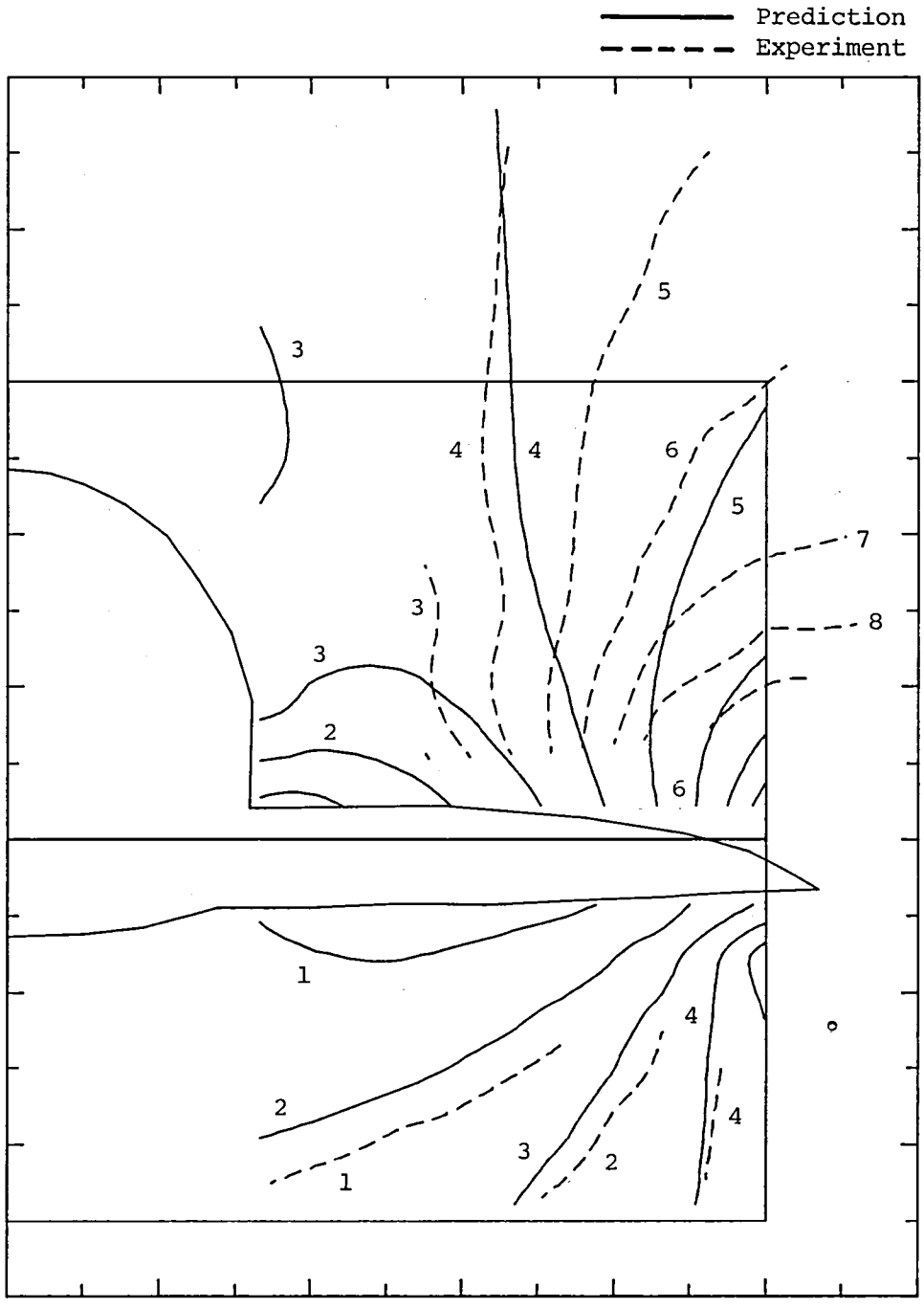

(a) α_l in degrees.

Figure 7.- Experimental contours and contours predicted by WIBCO at $M_\infty = 0.9$ and $\alpha = 5°$.

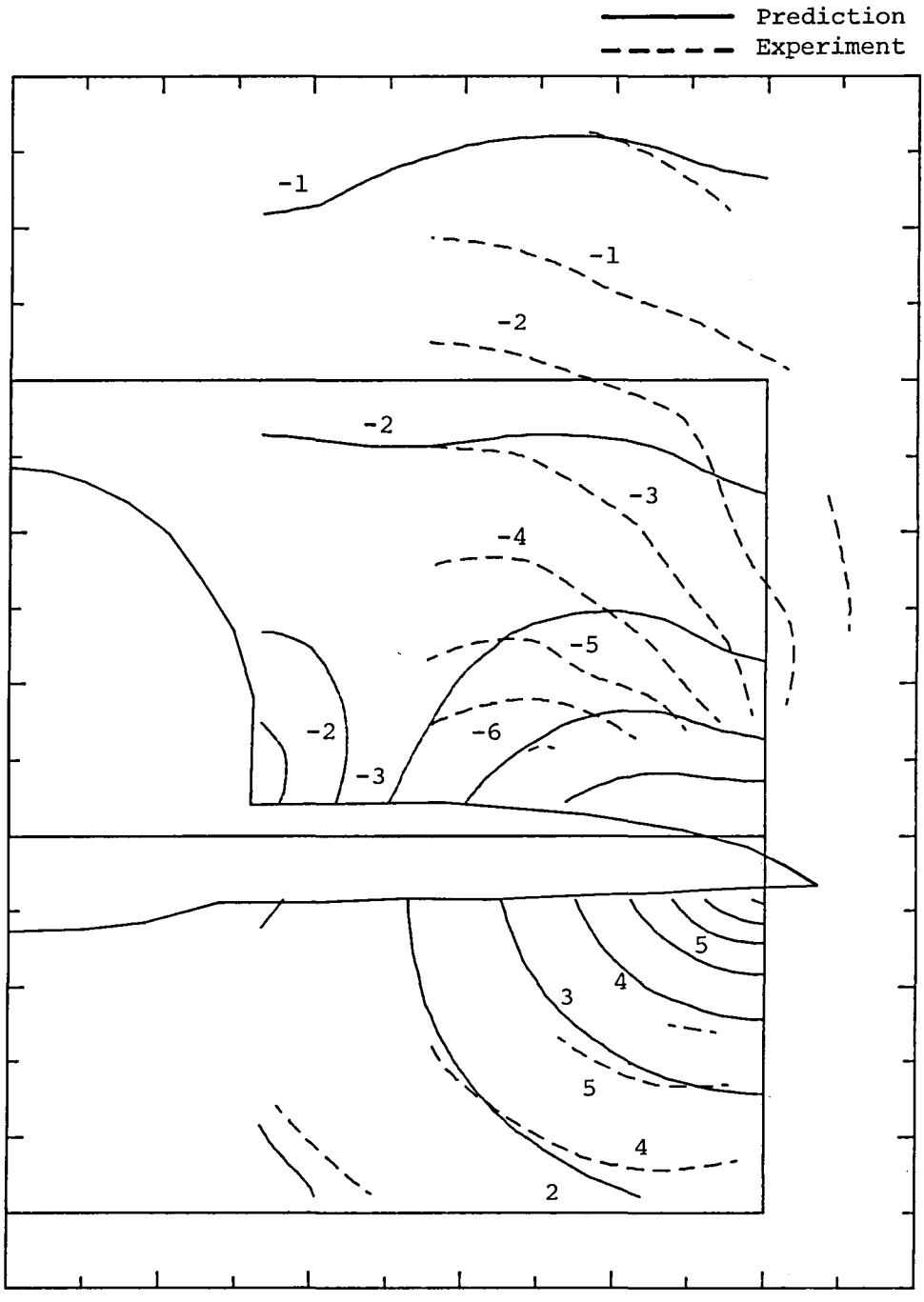

(b) β_1 in degrees.

Figure 7.- Continued.

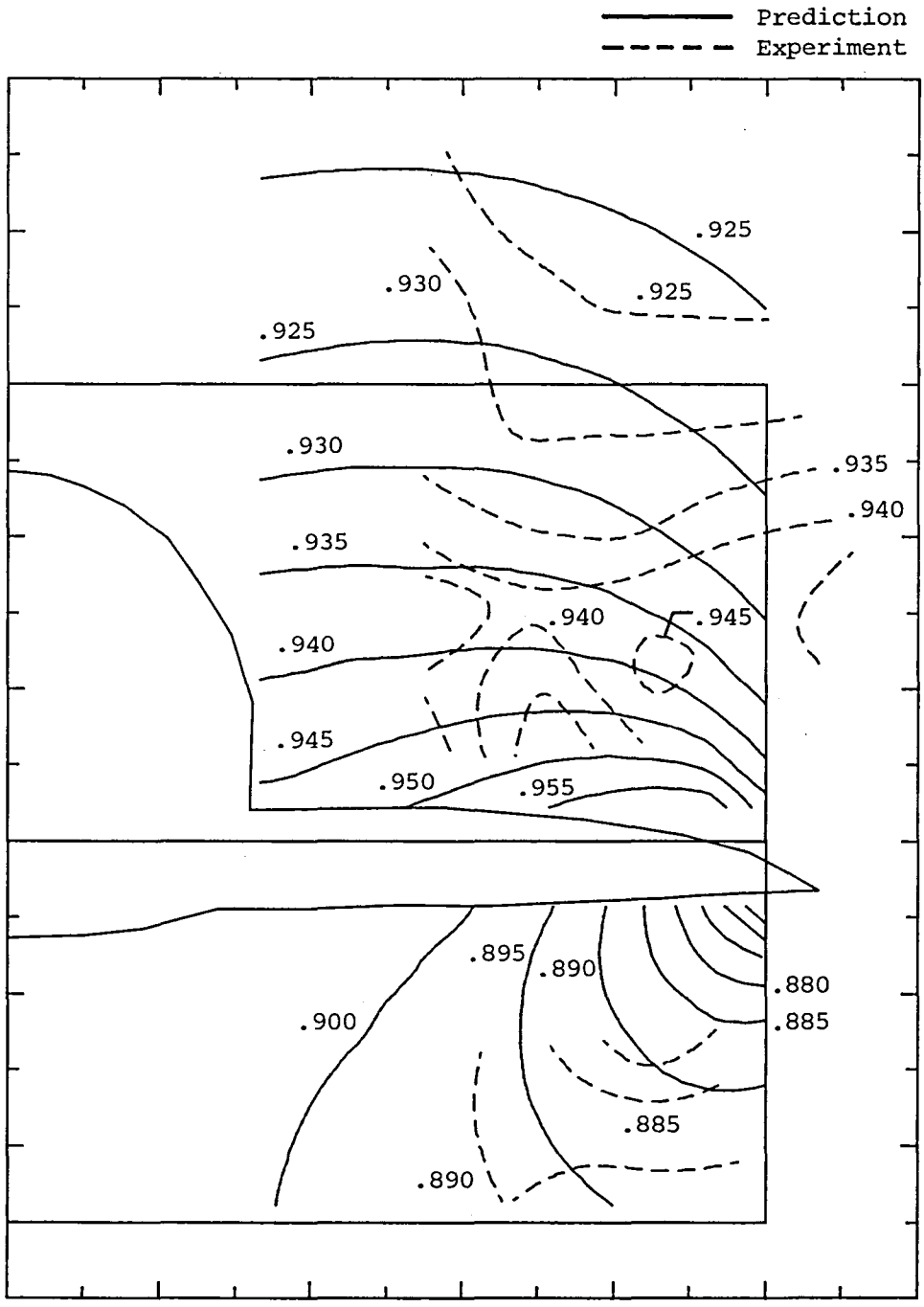

(c) M_1.

Figure 7.- Concluded.

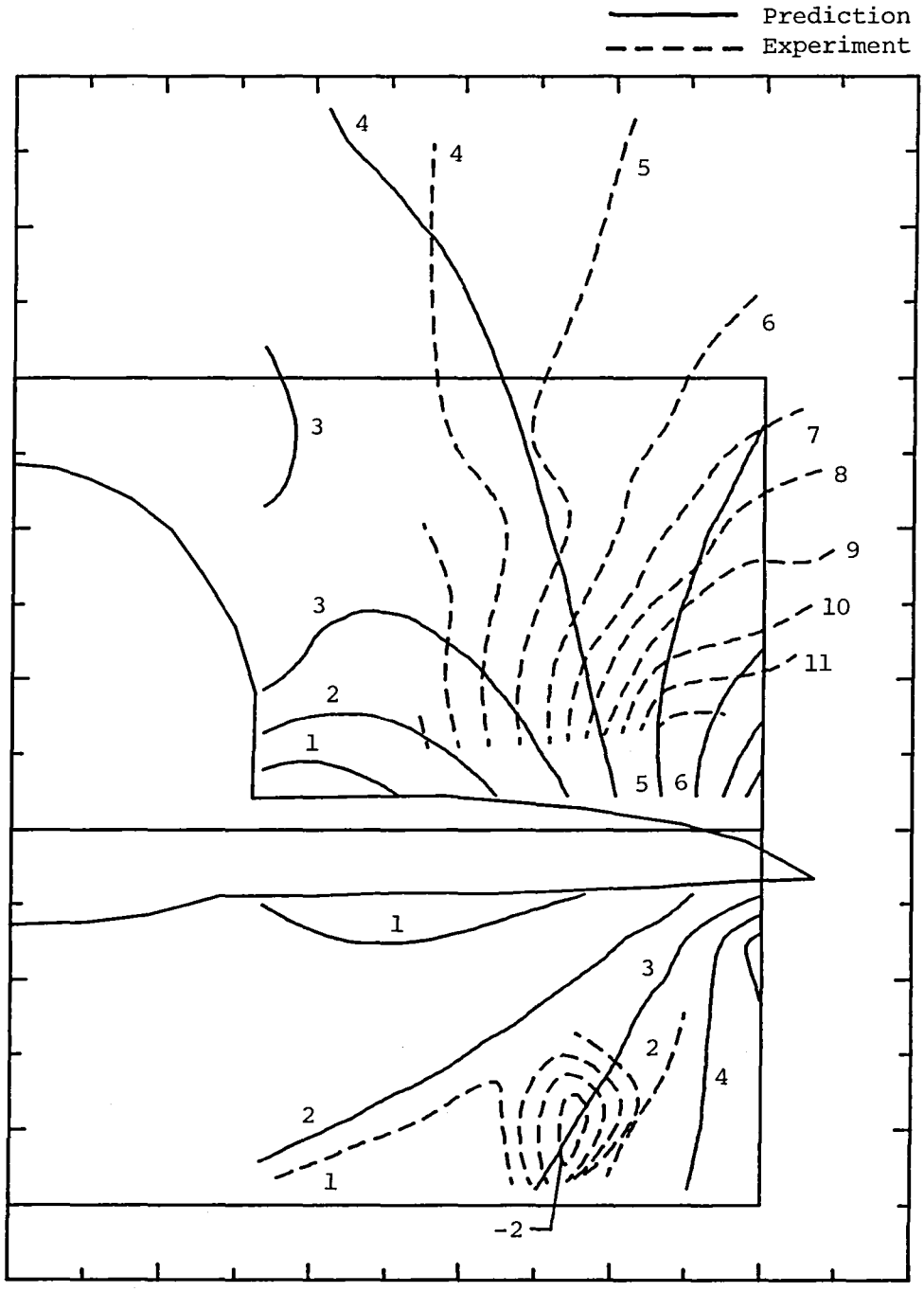

(a) α_l in degrees.

Figure 8.- Experimental contours and contours predicted by WIBCO at $M_\infty = 1.2$ and $\alpha = 5°$.

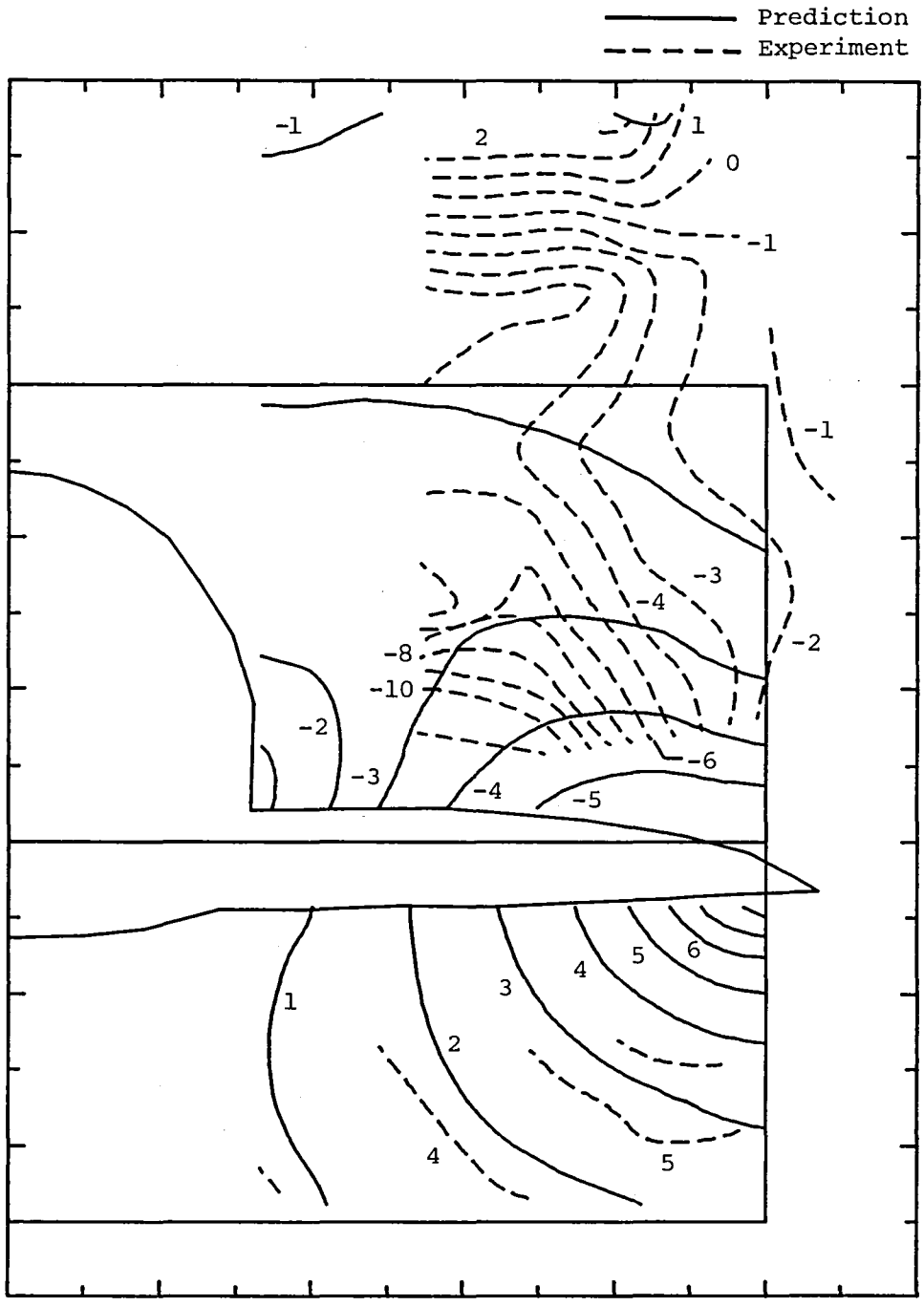

(b) β_1 in degrees.

Figure 8.- Continued.

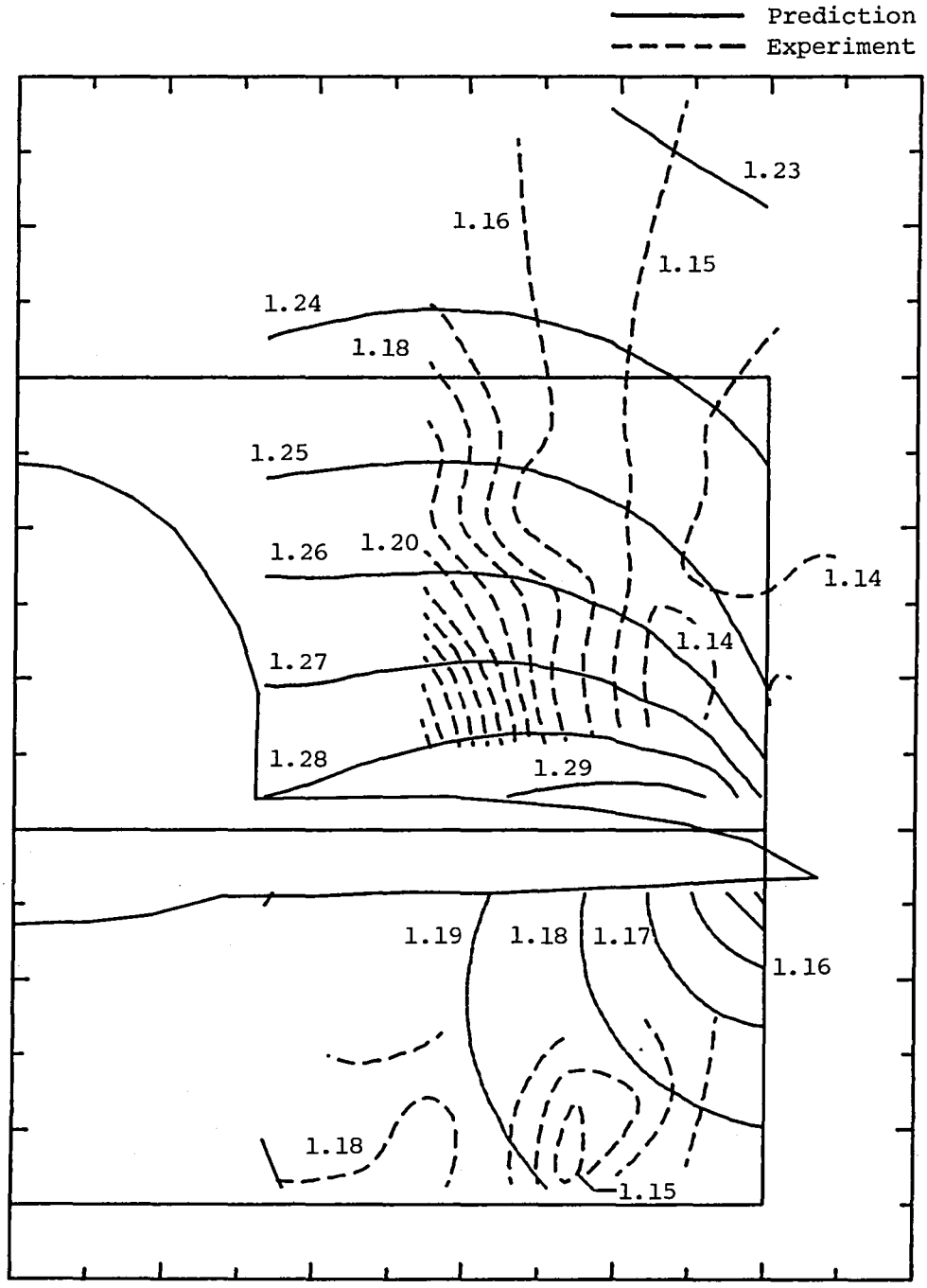

(c) M_1.

Figure 8.- Concluded.

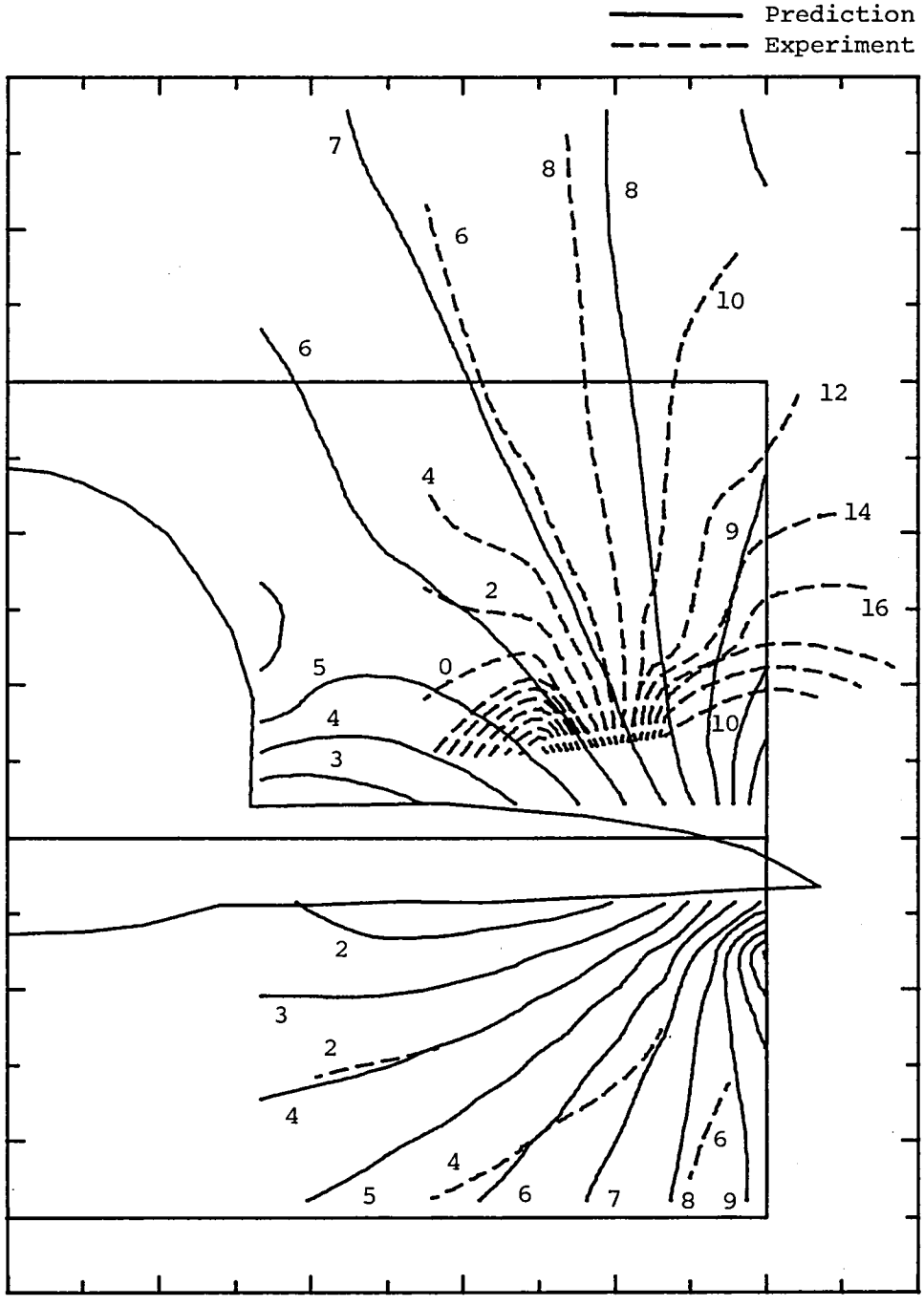

(a) α_1 in degrees.

Figure 9.- Experimental contours and contours predicted by WIBCO at $M_\infty = 0.6$ and $\alpha = 10°$.

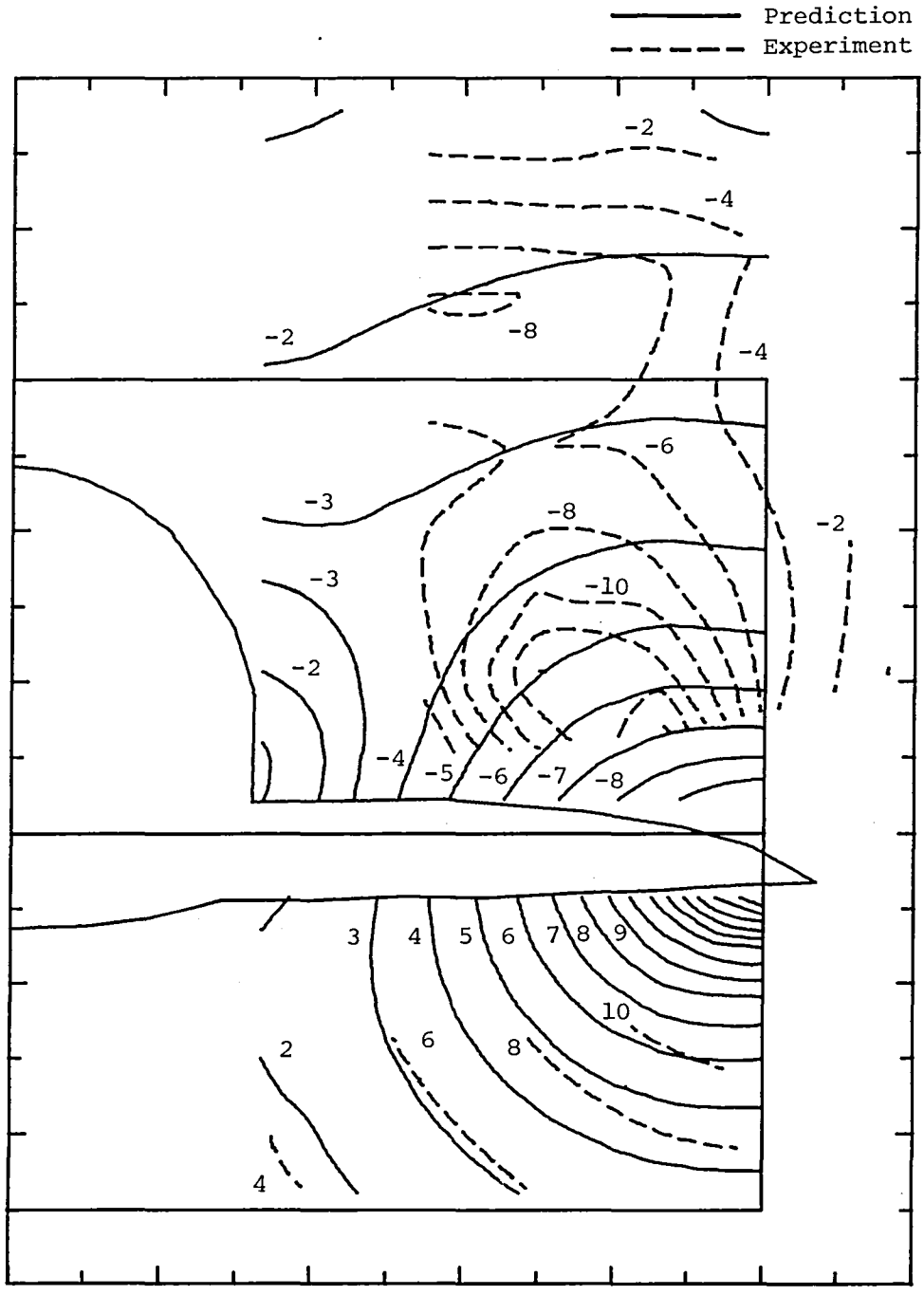

(b) β_l in degrees.

Figure 9.- Continued.

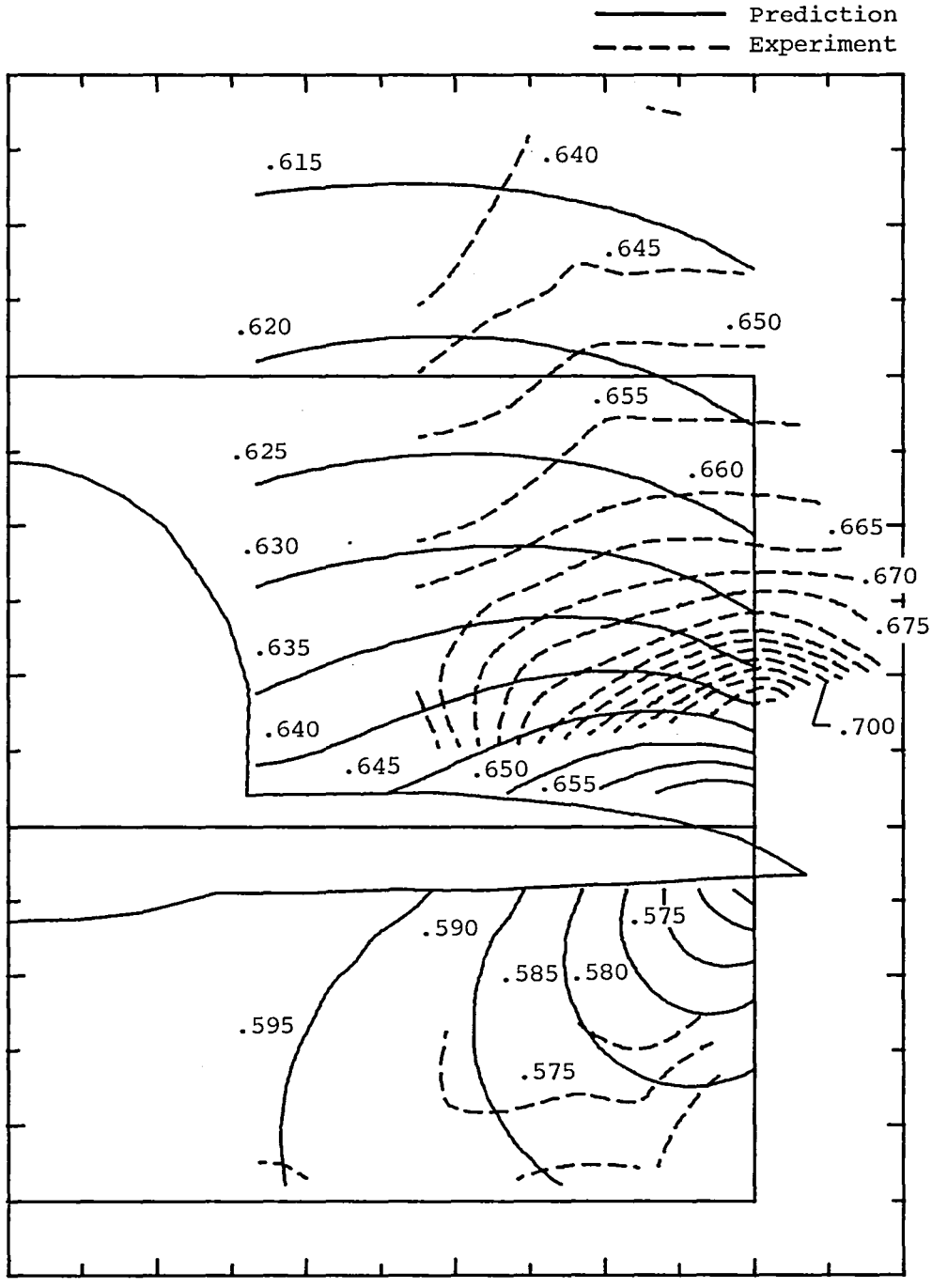

(c) M_l.

Figure 9.- Concluded.

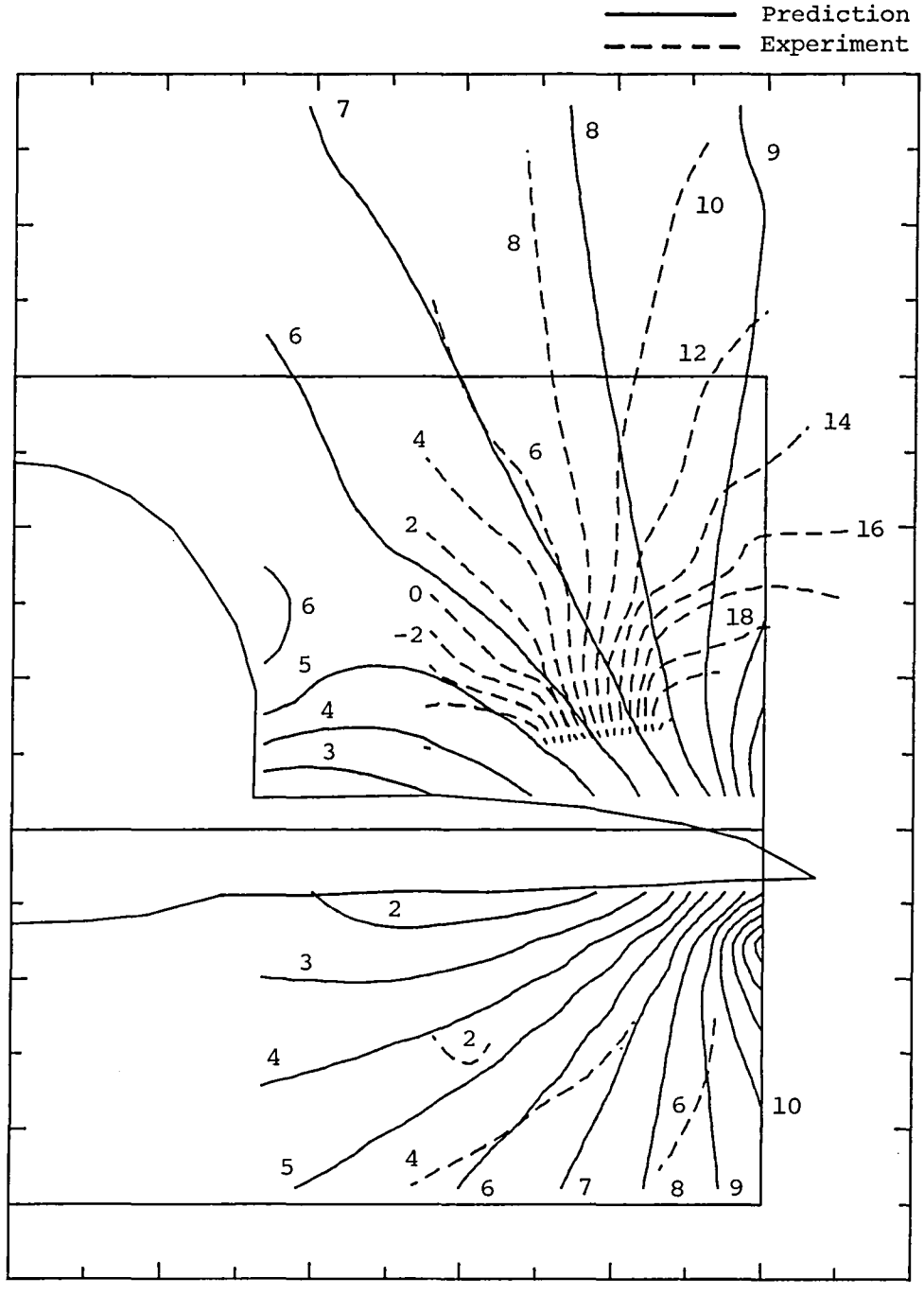

(a) α_l in degrees.

Figure 10.- Experimental contours and contours predicted by WIBCO at $M_\infty = 0.9$ and $\alpha = 10°$.

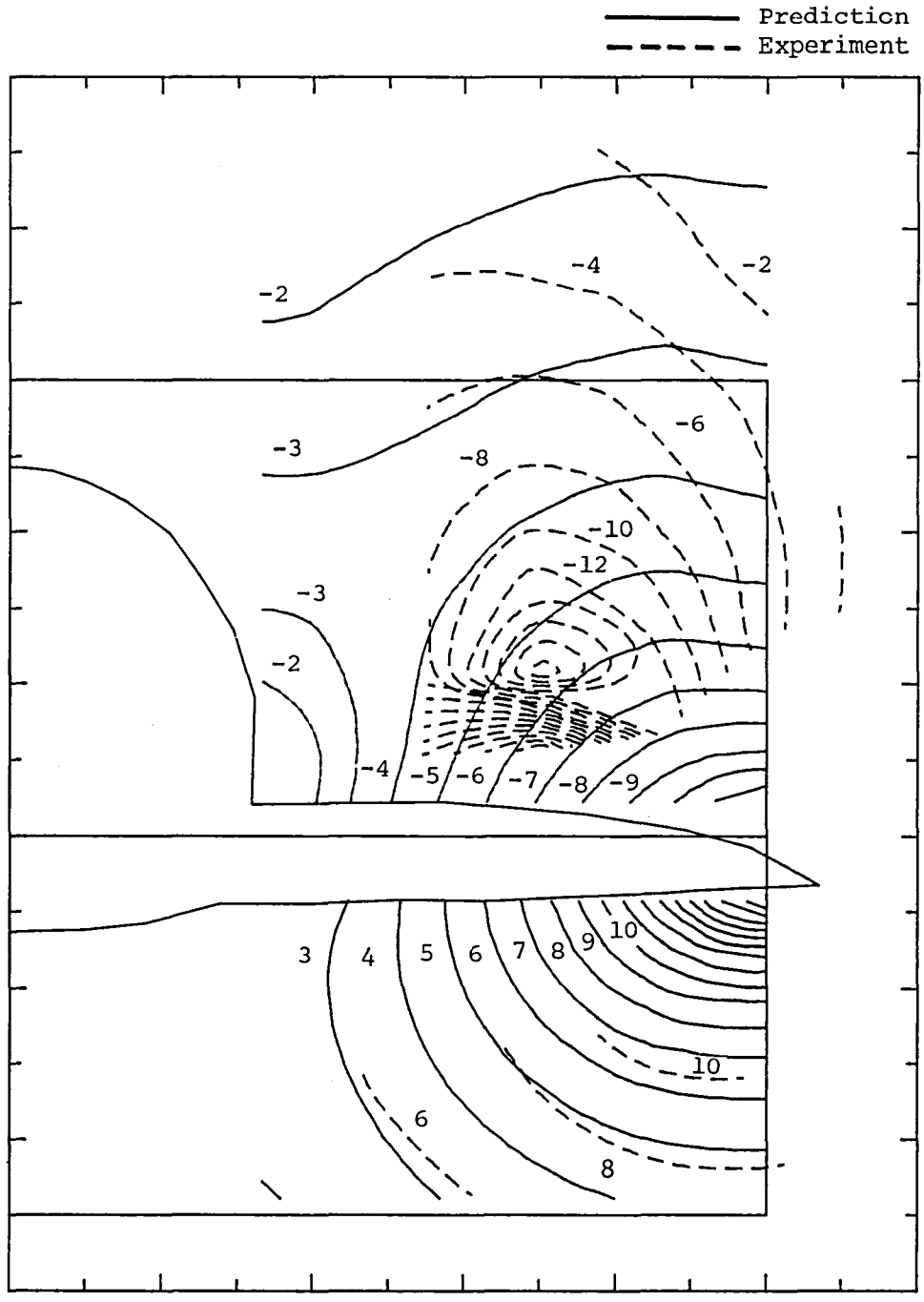

(b) β_1 in degrees.

Figure 10.- Continued.

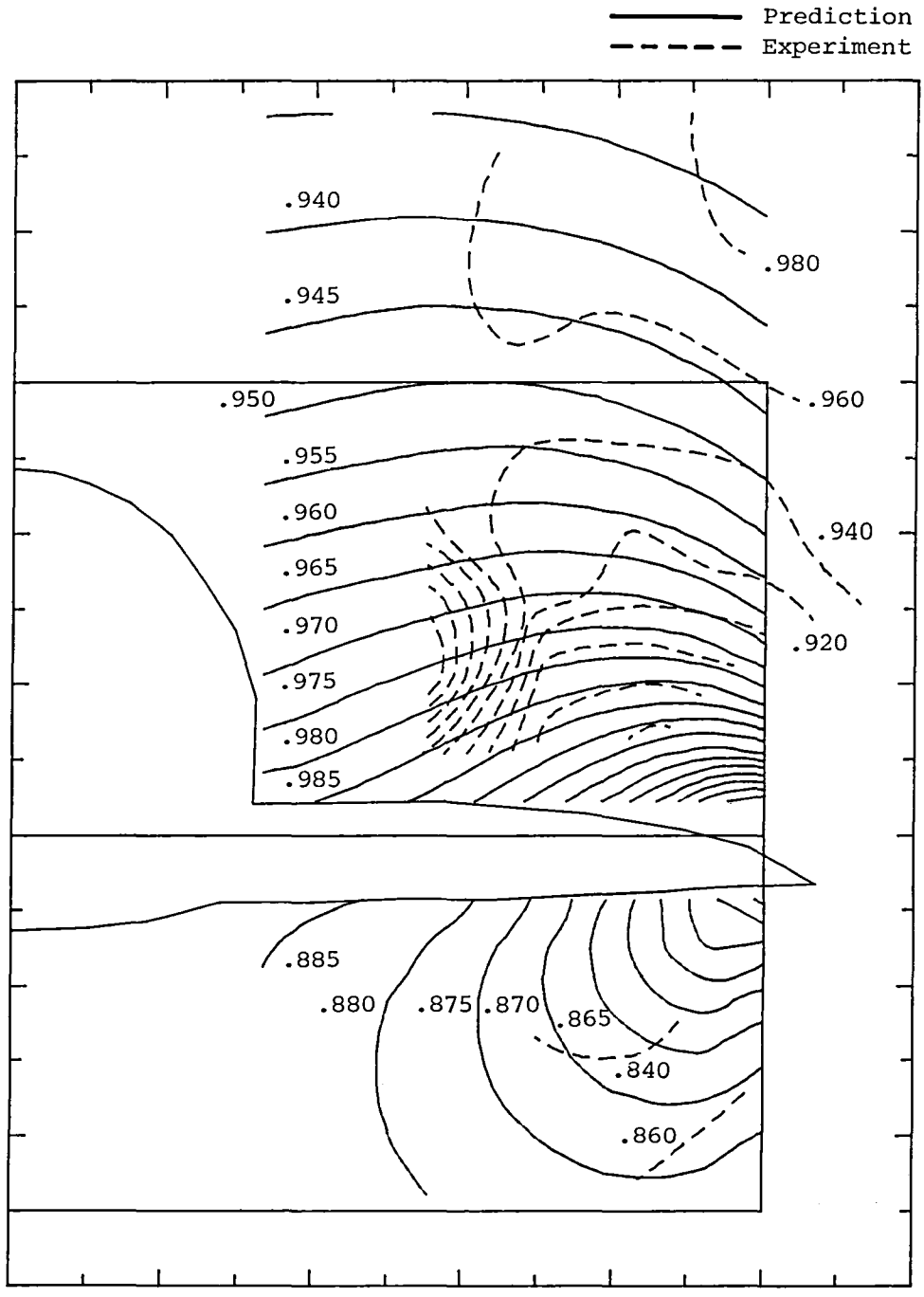

(c) M_1.

Figure 10.- Concluded.

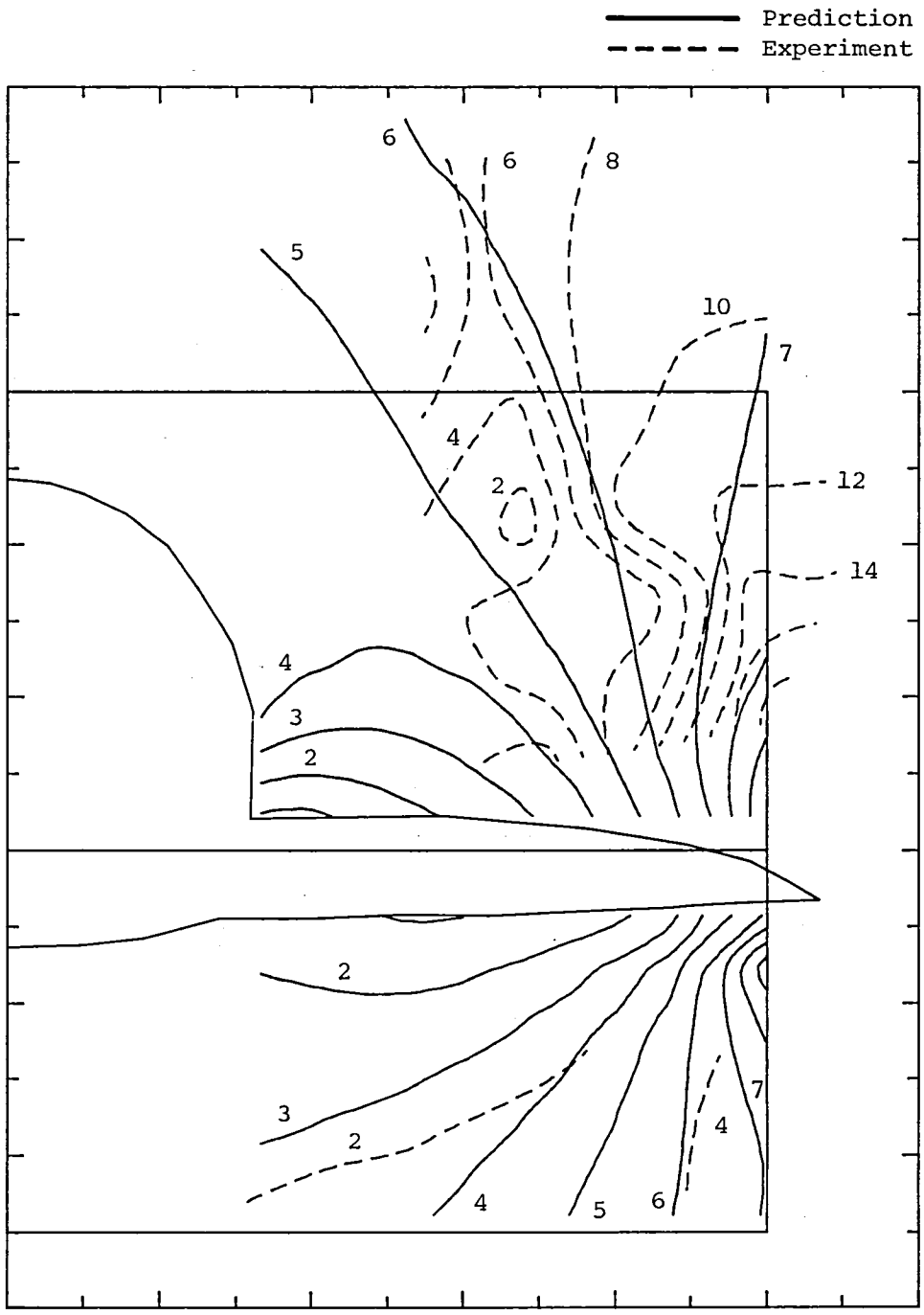

(a) α_l in degrees.

Figure 11.- Experimental contours and contours predicted by WIBCO at $M_\infty = 1.2$ and $\alpha = 7.5°$.

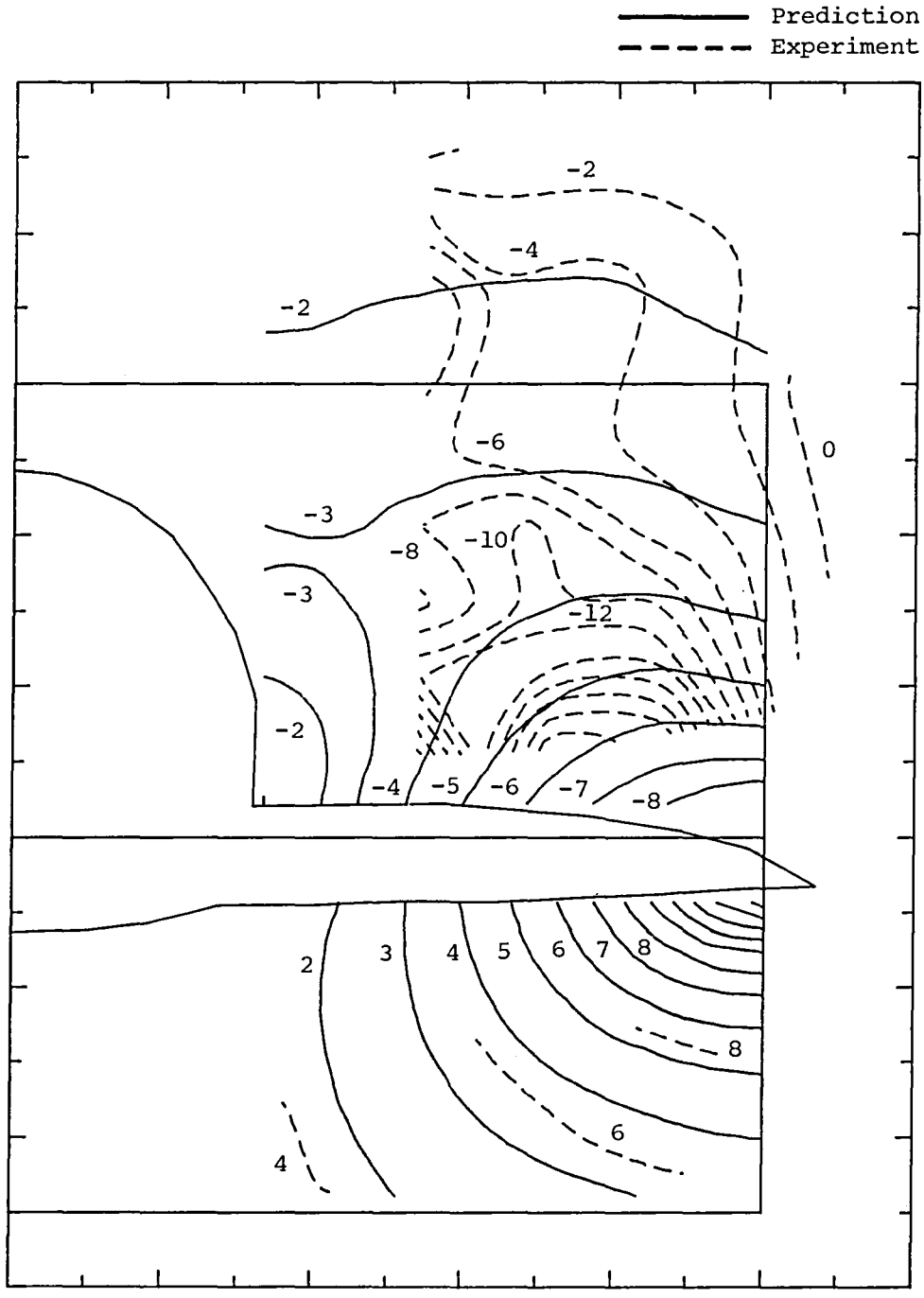

(b) β_1 in degrees.

Figure 11.- Continued.

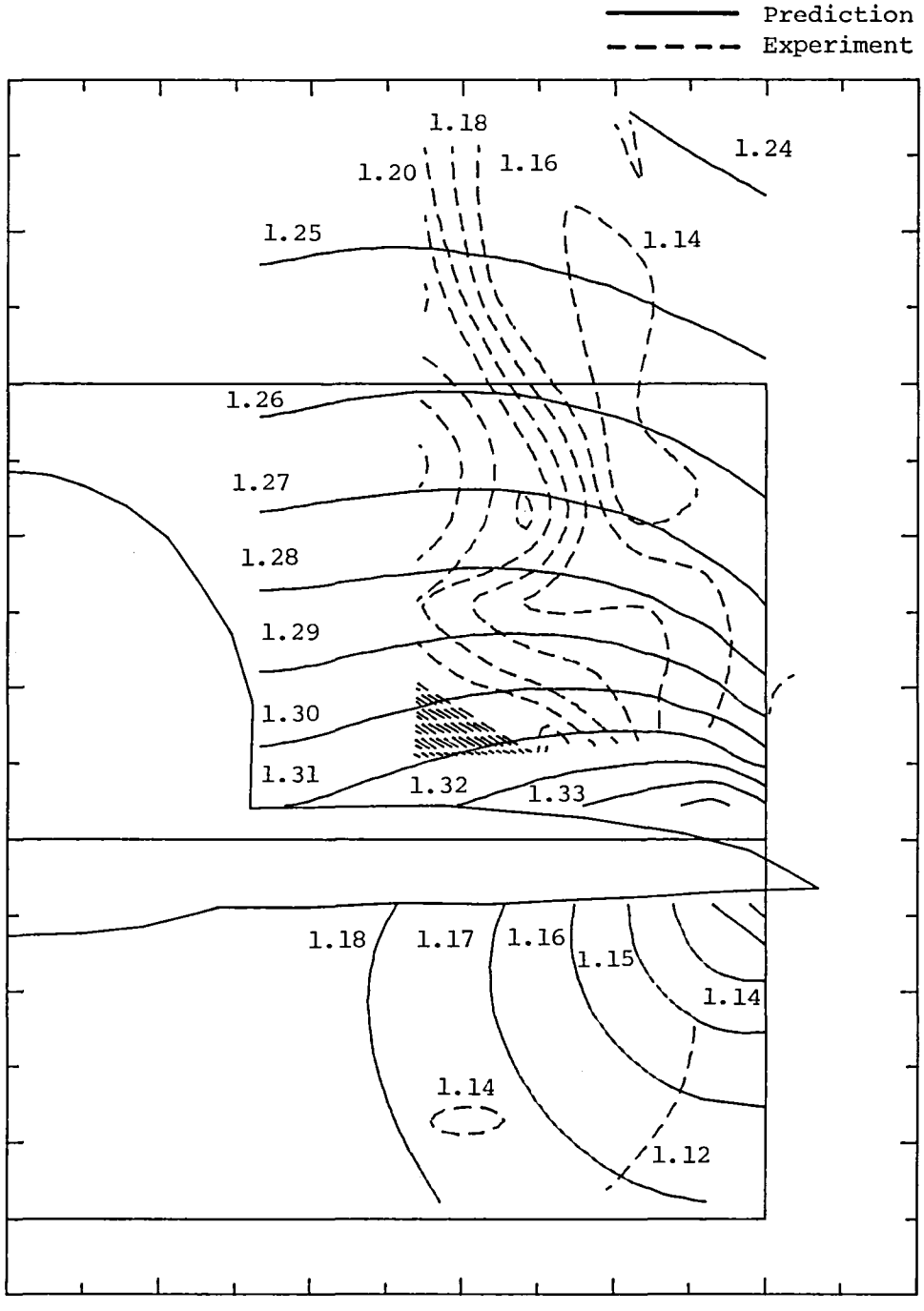

(c) M_1.

Figure 11.- Concluded.

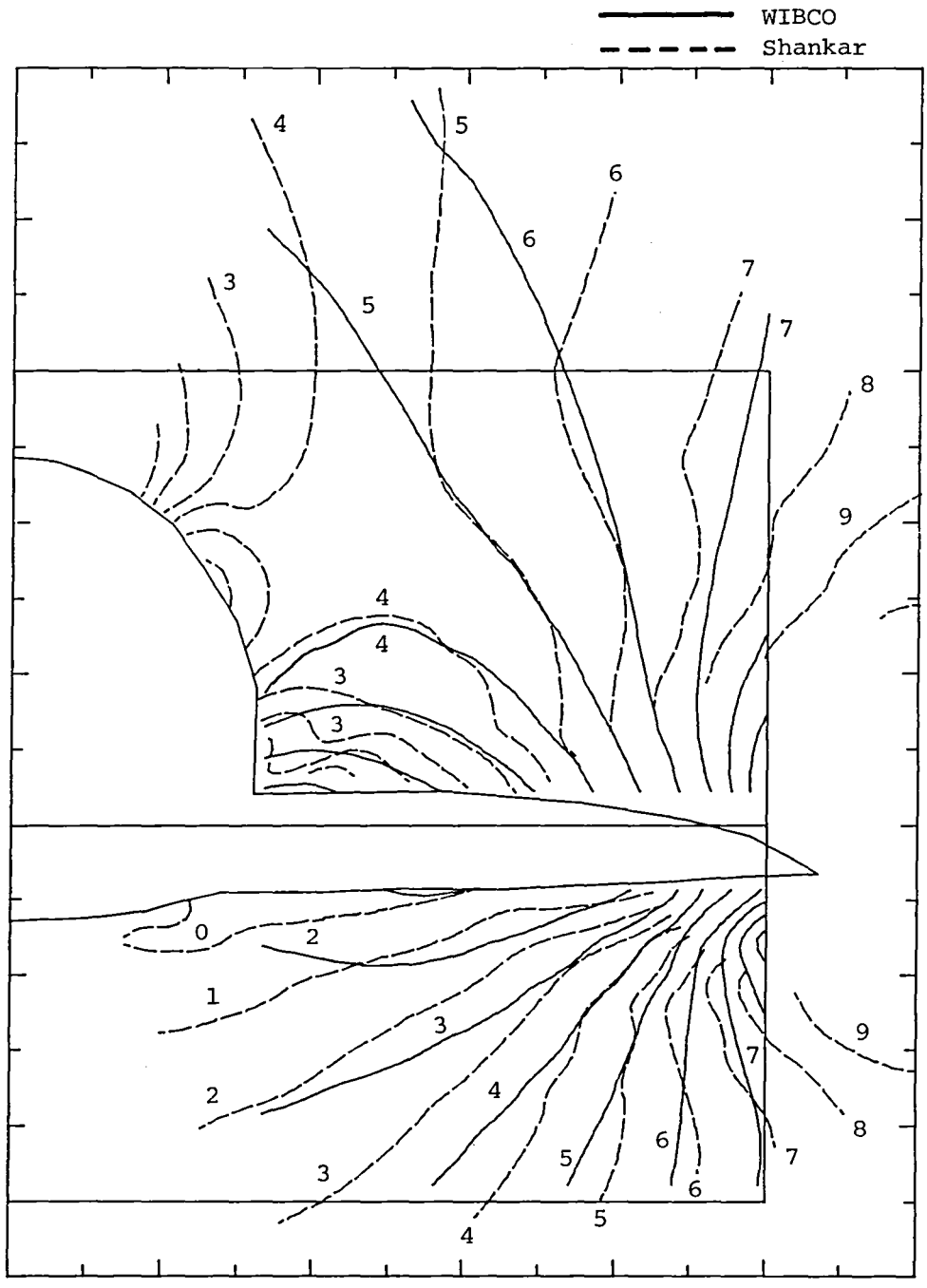

(a) α_l in degrees.

Figure 12.- Comparison of contours predicted by WIBCO and the Shankar code at $M_\infty = 1.2$ and $\alpha = 7.5^\circ$.

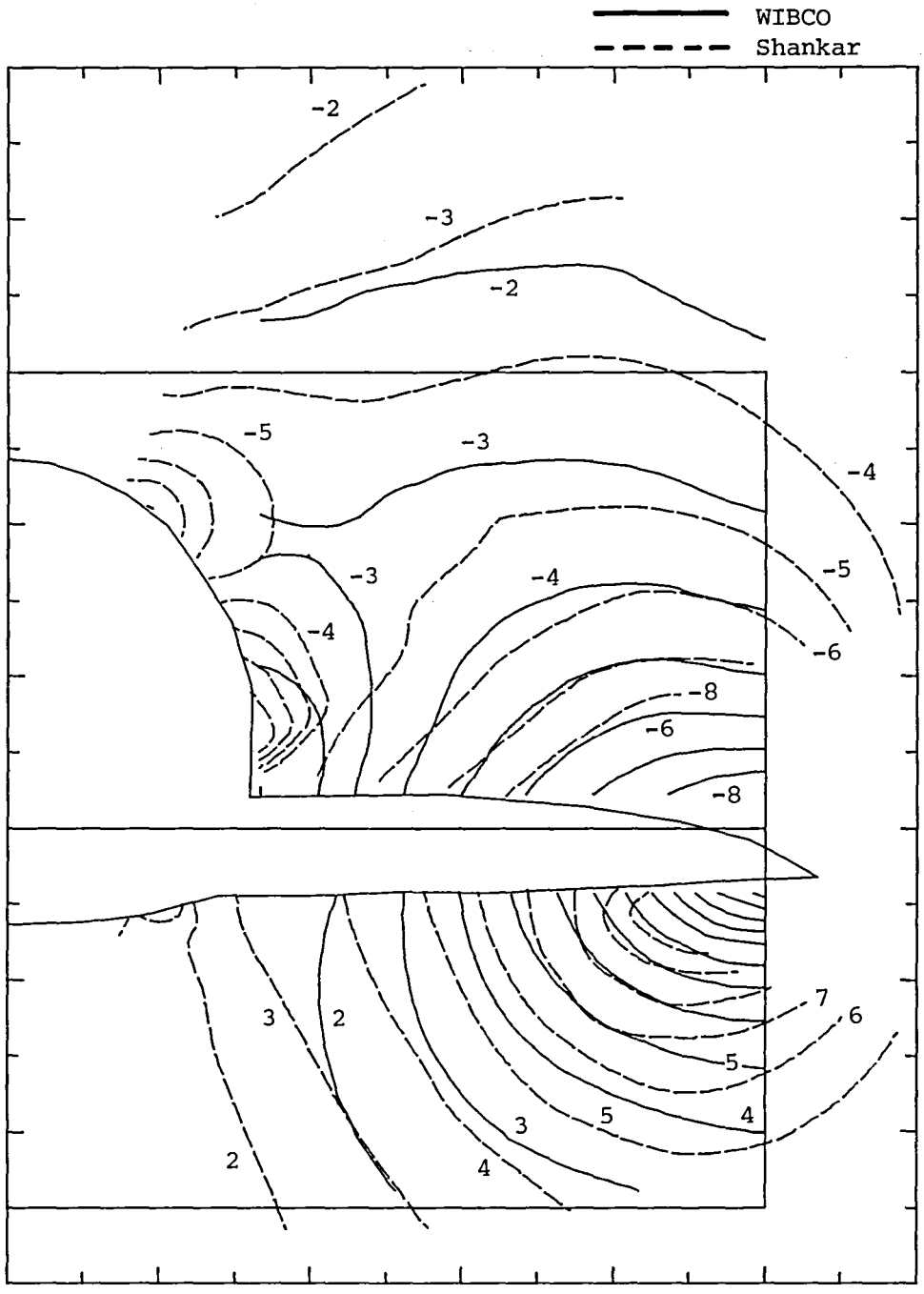

(b) β_1 in degrees.

Figure 12.- Continued.

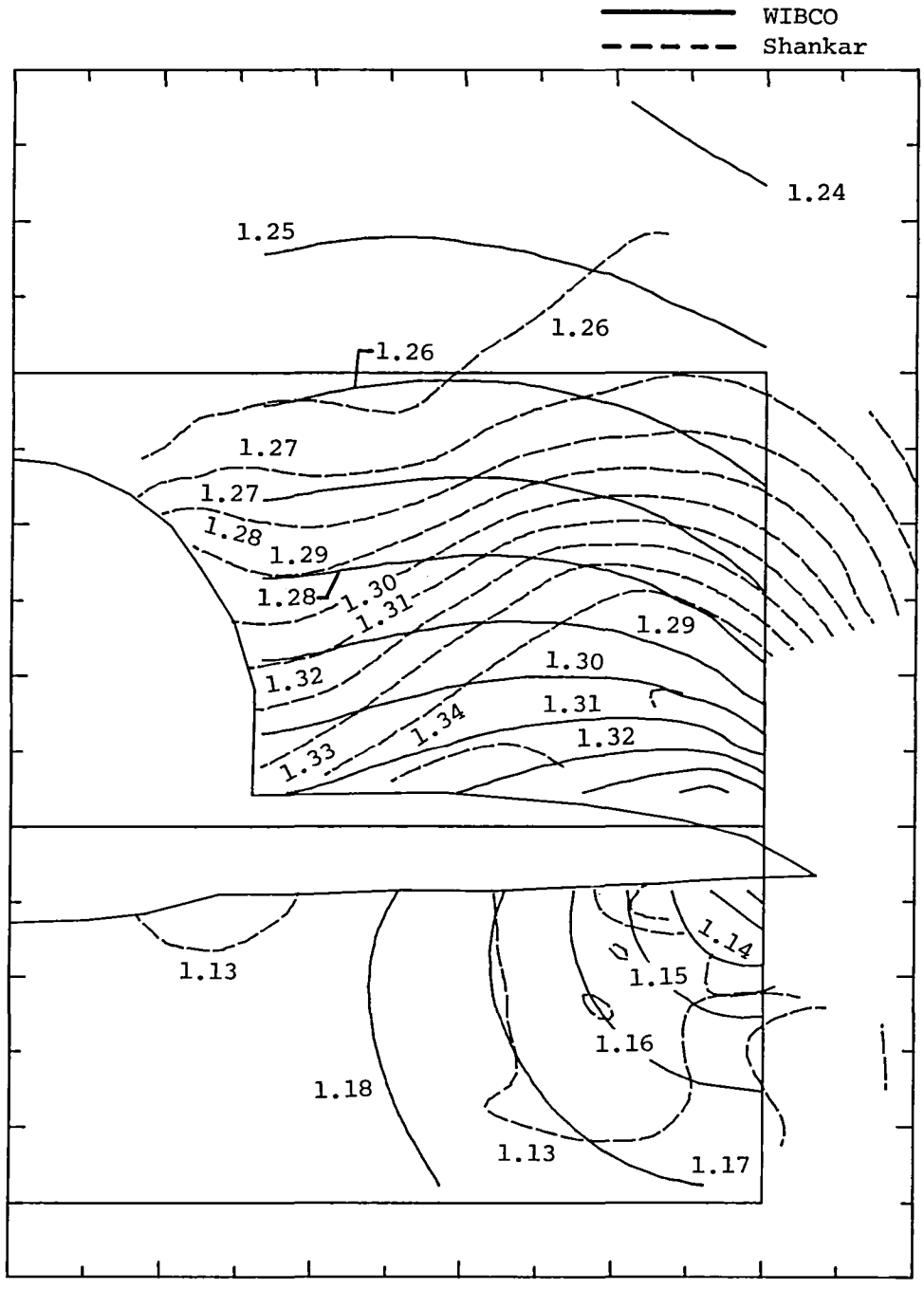

(c) M_1.

Figure 12.- Concluded.

1. Report No.	2. Government Accession No.	3. Recipient's Catalog No.
NASA TM-86450		

4. Title and Subtitle	5. Report Date
Theoretical and Experimental Flow Fields for a Supersonic Cruise Fighter Forebody	November 1985
	6. Performing Organization Code: 505-40-90-01
7. Author(s): Steven F. Yaros	8. Performing Organization Report No.: L-15914
9. Performing Organization Name and Address: NASA Langley Research Center, Hampton, VA 23665-5225	10. Work Unit No.
	11. Contract or Grant No.
12. Sponsoring Agency Name and Address: National Aeronautics and Space Administration, Washington, DC 20546-0001	13. Type of Report and Period Covered: Technical Memorandum
	14. Sponsoring Agency Code

15. Supplementary Notes

16. Abstract

This investigation examined the capability of two numerical methods to predict the flow field about a representative supersonic cruise aircraft. The two codes were a small-disturbance transonic program of Boppe and a conservative form full-potential transonic program of Shankar and Szema. For the former code, comparisons were made with wind-tunnel data at Mach numbers of 0.6, 0.9, and 1.2 and angles of attack of 0°, 5°, and 10° (7.5° instead of 10° at a Mach number of 1.2). Predictions from the two codes were compared at a Mach number of 1.2 and an angle of attack of 7.5°. The comparison criteria were contours of local angle of attack, local angle of sideslip, and local Mach number. The comparisons indicated that both codes may be considered useful for design applications, depending on the degree of accuracy required by the user's solution. Both solutions show an inaccuracy in their predictions, particularly as Mach number and/or angle of attack increases, because of their lack of viscous effects and any mechanisms to predict vortex development.

17. Key Words (Suggested by Authors(s))	18. Distribution Statement
Transonic flow Supersonic flow Forebody flow Supersonic cruise aircraft research	Unclassified - Unlimited Subject Category 02

19. Security Classif.(of this report)	20. Security Classif.(of this page)	21. No. of Pages	22. Price
Unclassified	Unclassified	41	A03

For sale by the National Technical Information Service, Springfield, Virginia 22161

NASA-Langley, 1985

End of Document